Shear Strength of Low-Rise Walls with Boundary Elements

By Felix Barda, John M. Hanson, and W. Gene Corley

Synopsis

Results of tests on eight specimens representing low-rise shear walls with boundary elements are reported and analyzed.

The principal variables included amount of flexural reinforcement, amount of horizontal wall reinforcement, amount of vertical wall reinforcement, and height-to-horizontal length ratio. Flexural reinforcement was varied from 1.8% to 6.4% of the boundary element area, horizontal wall reinforcement and vertical wall reinforcement were varied from 0 to 0.5% of the wall area, and height-to-horizontal length ratio was varied from 1/4 to 1.

The test program was designed to determine the effect of load reversals. Also, one specimen was repaired and retested.

Results indicate that current design procedures underestimate the strength of low-rise shear walls, even when the walls are subjected to reversed load. Finally, a suggested design procedure is presented

Keywords: cracking (fracturing); crack width and spacing; deflection; earthquake resistant structures; earthquakes; load tests (structural); reinforced concrete; reinforcing steels; repairs; shear strength; shear stress; shearwalls; structural design; walls.

---

[1]Lecturer, School of Civil Engineering, New South Wales Institute of Technology, Australia.

[2]Director, Structural Engineering Services, Wiss, Janney, Elstner, and Associates, Northbrook, Illinois.

[3]Director, Engineering Development Department, Portland Cement Association, Skokie, Illinois.

HIGHLIGHTS

Introduction

Previous investigations have developed information that describes the behavior of walls to resist lateral loads in high-rise buildings. However, little information is available concerning the behavior of walls for low-rise buildings.

Previous work showed that walls with a low height-to-horizontal length ratio have a higher unit shear strength than taller walls. However, no methods are available to predict this strength. Also, the relative contribution to shear strength provided by vertical and horizontal web reinforcement is not fully understood.

In the absence of definitive test data, many designers have assumed that the effect of load reversals is greater in low-rise walls, where shear strength may be expected to govern in design than in taller walls, where flexure usually governs. Similarly, little information is available concerning either reduction in stiffness due to load reversals or the ability of low-rise shear walls to absorb energy. Finally, the strength of a shear wall that has been repaired after it has been subjected to its ultimate load has not been reported in the literature.

Scope of the Investigation

The objective of this test program was to obtain data on the strength, energy absorption, performance under reversed loads, and serviceability of low-rise cast-in-place shear walls with boundary elements.

Dimensions of the test specimens are shown in Fig. 1. Each specimen was reinforced with Grade 60 deformed bars and contained normal weight concrete having a compressive strength of 3000 psi (211 kg per sq. cm). Measured strength of the concrete at test ranged from 2400 to 4200 psi (169 to 295 kg per sq. cm).

The horizontal length of the test walls was 75 in. (1.91 m) and the thickness was 4 in. (102 mm). Vertical boundary elements 24-in. (610 mm) wide and 4-in. (102 mm) thick were constructed at the extremities of the walls. These elements simulated cross walls or columns in a real structure and contained bars that acted as flexural reinforcement. The amount of flexural reinforcement was varied from 1.8 to 6.4% of the area of the vertical boundary elements. Vertical and horizontal

reinforcement used in the wall was varied from 0 to 0.5% of the area of the wall.

Each specimen was topped with a slab 60-in. (1.52m) wide and 6-in.(152mm)thick simulating a floor or roof element. A large base simulating a heavy footing was prestressed to the laboratory floor.

Six test specimens had a height-to-horizontal length ratio of 1/2. Two specimens had height-to-horizontal length ratios of 1/4 and 1. Two of the specimens with a height-to-horizontal length ratio of 1/2 were subjected to load reversals representing a severe seismic loading. As illustrated in Fig. 1, the loads were applied to the wall through the top slab. Loading was continued after the ultimate shear was reached, until a deflection of 3 in. from center was attained.

Findings and Conclusions

1. Shear strength of the test specimens was not affected by differences in the amount of flexural reinforcement, so long as all bars are properly anchored to the foundation.

2. A nearly orthogonal pattern of cracking developed in the specimens subjected to load reversals. This cross-cracking did not greatly affect the behavior of the specimens.

3. Specimens subjected to load reversals had a shear strength about 10% less than similar specimens subjected to loading in one-direction.

4. A shear wall that was damaged in one test was effectively repaired by recasting loose and spalled concrete. After being repaired, its shear strength when it was retested was reduced by 20%. However, energy absorption of the repaired wall was higher than that of the original wall.

5. For the specimens with a height-to-horizontal length ratio of 1/2 and less, it was found that horizontal wall reinforcement did not contribute to shear strength. However, the horizontal bars were effective in producing a more distributed cracking pattern and in reducing crack widths. The observations

led to the recommendation that minimum horizontal reinforcement should be provided in all walls.

6. Vertical wall reinforcement was effective as shear reinforcement in the specimens with a height-to-horizontal length ratio of 1/2 and 1/4. However, it was less effective in the specimen with a height-to-horizontal length ratio of 1. Vertical bars were also effective in producing a distributed crack pattern and in reducing crack widths. These observations led to the recommendation that minimum vertical reinforcement should be provided in all walls.

7. The presence of the top slab appeared to have a significant influence on the shear strength of the specimens with a height-to-horizontal length of 1/2 and 1/4. This suggests that the behavior of piers and spandrels might differ from that of low-rise walls.

8. Shear strength of a specimen with a height-to-horizontal length ratio of 1/4 was not significantly higher than the shear strength of a comparable specimen with a height-to-horizontal length ratio of 1/2.

9. Shear strength of a specimen with a height-to-horizontal length ratio of 1 was about 20% lower than the shear strength of comparable specimens with height-to-horizontal length ratios of 1/2 and 1/4.

10. Slip or other distress at construction joints at the bottom and top of some walls may have slightly reduced their strength. However, joint slip appeared to have the beneficial effect of increased energy absorption.

11. Shear force was observed to be transmitted from the top slab to the base through the formation of compressive "struts" in the wall between cracks. For the specimens with a height-to-horizontal length ratio of 1/2, these struts were inclined at about 38 degrees.

12. The behavior of the specimens was observed to be similar to that of deep beams and corbels. A specimen containing no shear reinforcement had a shear strength above the stress associated with first shear cracking. Application of load through the top slab rather than directly to the wall as has been done in deep beam and corbel tests did not appear to influence the results.

13. Load-carrying capacity beyond maximum load depends primarily on the ability of the boundary elements to act as a frame. In all cases, the frame action provided a mode of failure that was gradual rather than sudden and catastrophic.

14. Shear strength of low-rise walls can be evaluated in terms of current design practice that attributes part of the strength to the concrete and the rest to the wall reinforcement. A revised equation for calculating v_c for low-rise walls is presented.

BACKGROUND

In early studies of shear capacity of beams, it was observed that shear reinforcement is not stressed until diagonal tension cracks occur. Once cracks occurred, force in the reinforcement accounted for less than the total shear on a beam. This observation led to the concept that shear capacity can be divided into two parts: the shear carried by the concrete, and the shear carried by web reinforcement. Background information on this concept and on how it was incorporated into the 1963 and 1971 ACI Building Codes[1-2] is reported elsewhere[3-5].

Beginning in the 1960's, several experimental investigations[6-12] of deep beams were conducted. Deep beams are defined as members with a span-to-depth ratio of less than about 5. The results of these tests demonstrated that diagonal cracking occurs in deep beams at about the same nominal shear stress as in ordinary beams. However, unlike ordinary beams that exhibit little post-cracking strength, deep beams may be able to carry 3 to 4 times the shear that caused diagonal cracking. It

was also found that the addition of vertical reinforcement or horizontal reinforcement or both in the web region further increases shear capacity.

Shear walls differ from deep beams in several important respects. First, they are generally very thin members that may fall into the classification, based on the length of "shear span", of either an ordinary beam or a deep beam. The "shear span" is defined as the ratio of moment to shear at a critical section. In most laboratory tests, if dead load is neglected, the shear span is the distance from a simple support to the closest concentrated load. Second, loads are assumed to be transmitted to deep beams at points on their top or bottom surface by columns while loads applied to shear walls are normally distributed along floor lines.

Tests of specimens that simulate details and loadings of shear walls was carried out in the 1950's at Stanford University and at MIT[13-19]. Based on the tests, equations for predicting the capacity of shear walls subject to dynamic and static loads were developed. These equations are restricted to the range of variables tested.

In 1967, the Portland Cement Association undertook an extensive test program[20-21]. A total of thirteen large specimens representing shear walls with rectangular cross-sections were tested.

Results of the PCA tests indicate that the flexural strength of rectangular shear walls for high-rise buildings can be predicted from assumptions satisfying compatibility of strains across the cross-section. Furthermore, it was found that the strength of tall shear walls containing minimum horizontal reinforcement will generally be controlled by flexure. For low-rise walls, both horizontal and vertical reinforcement contributed to the shear strength. The capacity of one specimen subjected to load reversals was essentially the same as a similar specimen subjected to load applied in one direction.

Special provisions for shear walls, based on the research carried out at the Portland Cement Association, at MIT and at Stanford University were included in the 1971 ACI Building Code[2].

EXPERIMENTAL INVESTIGATION

Description of Test Specimens

The test specimens, illustrated in Fig. 1, were intended to represent shear walls for low-rise buildings. The horizontal length, ℓ_w, was 75 in. (1.91 m). This is the same length used in earlier test programs carried out at the Portland Cement Association[20-21]. The web thickness, h, was 4 in. (102 mm). Vertical boundary elements or flanges 24-in. (610 mm) wide and 4-in. (102 mm) thick, were built-in at the ends of each wall. These elements simulated cross walls or columns in a real structure.

The top edge of each wall was built into a slab 60-in. (1.52 m) wide and 6-in. (152 mm) thick. This slab was intended to represent a floor or roof. A large monolithic base supported each wall. During testing, the base was prestressed to the laboratory floor.

Load was applied to the top slab in the manner shown in Fig. 1. This scheme was intended to simulate the distribution of shear forces at the interface of a floor slab and shear wall in a prototype structure.

The height, h_w, to horizontal length, ℓ_w, ratio was a variable in this investigation. To obtain this variation, all dimensions except h_w were kept constant in all the specimens. Horizontal construction joints were used at the junction of the base and the wall, and at the junction of the top slab and the wall. The height of each specimen and the amount of wall and flange reinforcement are listed in Table 1.

The test specimens were made with concrete having a design compressive strength of 3000 psi (211 kg per sq. cm) at 28 days. The maximum size of coarse aggregate was 3/4 in. (19 mm). Although this maximum size is larger than that required by consideration of scale, it was selected because it is representative of aggregate used in full-size buildings. With this size aggregate and a web thickness of 4 in. (102 mm), it was possible to place the wall reinforcement in two layers. This is representative of common reinforcement details. Properties of the concrete are summarized in Table 2.

Representative horizontal and vertical cross-sections through the wall are shown in Figs. 2 and 3, respectively. The horizontal and vertical wall reinforcement was anchored in the boundary elements. Development lengths complied with the requirements of the 1971 ACI Building Code[2]. The design yield stress of the reinforcement was 60,000 psi (4220 kg per sq.cm). Measured properties of the reinforcement are presented

in Table 3.

The flanges contained sufficient flexural reinforcement to provide a moment capacity larger than the shear strength. They were detailed to meet requirements of "Appendix A - Special Provisions for Seismic Design" of the 1971 ACI Building Code[2].

Each specimen was cast in three operations. First the base was cast, then the wall, and finally the top slab. After placing and vibrating the base concrete, a 3/8-in. (9.5 mm) diameter blunt-ended rod was used to roughen the construction joint at the wall. A pattern of small holes approximately 3/8-in. (9.5 mm) deep was rodded into this and all other construction joints.

One batch of concrete was required to cast the wall of Specimen B7-5, four batches were required for Specimen B8-5. For all other specimens, two batches were required. After placing and vibrating the wall concrete, the top surface at the joint with the top slab was roughened in the same way as the joint between the base and the wall. After the top slab was cast, it was covered with a polyethylene sheet for curing. Three days after casting the slab, forms were removed. Wall concrete was generally four to seven days old at that time.

In preparation for testing, the specimens were painted with a thin coat of oil base flat paint. The paint was applied to make cracks more readily visible during testing. The specimens were lifted off the wooden platform and positioned in a large prestressed concrete loading frame. A portland cement and sand grout pad approximately 1/2-in (12.7 mm) thick was used to level the specimens on the laboratory floor. After the grout had set, the base was prestressed to the laboratory floor at eight points.

Load was applied by two 100-ton hydraulic rams. The rams transmitted their forces to the specimen through a 2-in. (50.8 mm) thick steel bearing plate. The system was designed to be both self-supporting and self-aligning during load reversals.

The loading system contained a valve in the hydraulic line. When a desired load level was reached, the valve was closed, thereby holding a constant volume of oil in the loading system. This provided control of lateral deflection at each load stage.

Wire filament electrical resistance strain gages were attached at selected locations using procedures

described elsewhere[23]. One-quarter of the main flexural reinforcing bars was gaged at the base, at mid-height, and at the top of the wall. Six vertical web bars were gaged at the base, at mid-height, and at the top of the wall. This pattern gave both distribution of vertical strains along the horizontal length of the walls and along the bars. Selected horizontal web bars were each gaged at 5 locations. This pattern of gaging gave the distribution of horizontal strains at five different vertical sections, as well as the distribution along the gaged bars.

All strain gages were connected to a VIDAR digital data acquisition system. This system records measured information on both printed and punched tape at the rate of 10 channels per second.

Lateral deflection of the top of the specimens was measured by two electrical resistance potentiometers, and one direct current differential transformer (DCDT). One of the potentiometers and the DCDT were connected to the VIDAR system. The other potentiometer was connected to an X-Y plotter. Additional deflection measurements were obtained with a dial gage and a theodolite sighting on a scale.

Three DCDT's and four potentiometers connected to the VIDAR were used to measure the vertical and lateral deformation of the underside of the top slab at the flanges and at the mid-length of each specimen.

Two linear variable differential transformers (LVDT) were connected between the underside of the top slab and the base of each specimen at the boundary elements. The LVDT's were directly connected to an X-Y plotter to measure the rotation of the top slab.

Two load cells, each consisting of a metal tube with strain gages attached[23-24], were used to measure the applied force in each direction of loading. One of the load cells was connected to the VIDAR system, the other to two X-Y plotters. The plotters were used to continuously record load versus lateral deflection at the top of the wall, and moment versus rotation of the top slab.

Potentiometers were used to measure slip at the top and bottom construction joints. At each joint, potentiometers were placed at each flange, and at mid-length of the wall. These potentiometers were also connected to the VIDAR.

At selected load stages, crack widths were measured by means of a 50 power microscope.

Black and white prints and 35mm color slides were used to obtain a record of the change in the crack patterns as the specimens were loaded. Photographs were generally taken at every significant change in the crack pattern.

Test Program

The test program was divided into 5 phases as listed in Table 4. In Phase 1, Specimens B1-1 and B2-1 were tested to determine the effect of varying the amount of flexural reinforcement. These specimens, both with a height-to-horizontal length ratio of 1/2, were subjected to loads applied in one-direction only. All other walls were subjected to load reversals.

The amount of flexural reinforcement used in Specimen B1-1 was 1.8% of the area of the flanges. This specimen was expected to have a flexural capacity slightly greater than its shear capacity. A larger amount of flexural reinforcement, equal to 6.4% of the area of the flanges, was used in Specimen B2-1.

Specimens B1-1 and B2-1 contained 0.5% vertical and horizontal reinforcement in the wall. Based on the provisions in Section 11.16 of the 1971 ACI Building Code [2], this amount of reinforcement would resist a nominal shear stress, v, of $5.5\sqrt{f'_c}$ psi. With an expected concrete contribution of about $3.3\sqrt{f'_c}$ psi, the predicted shear strength of these specimens was $8.8\sqrt{f'_c}$ psi.

In Phase 2, Specimen B3-2 was tested under reversed application of load. Its behavior was compared with that of Specimens B1-1 and B2-1 in Phase 1 to determine the effect of repeated load reversals. Specimen B3-2 contained the same amount of wall reinforcement and had the same height, h_w, as Specimens B1-1 and B2-1. However it contained flexural reinforcement equal to 4.1% of the area of the flange.

In Phase 3, Specimen B4-3 was identical to Specimen B3-2, except that it contained no horizontal web reinforcement. Behavior of Specimen B4-3 was compared with that of Specimen B3-2 to determine the effect of different amounts of horizontal web reinforcement.

In Phase 4, Specimens B5-4 and B6-4 were identical to Specimen B3-2, except for the amount of vertical web reinforcement. Behavior of Specimens B5-4 and B6-4 was compared with that of Specimen B3-2, to determine the effect of different amounts of vertical web reinforcement.

Specimens B5-4 and B6-4 contained no vertical web reinforcement and 0.25% vertical web reinforcement, respectively. Although Specimens B5-4 and B6-4 also contained 0.5% horizontal web reinforcement, they did not comply with the minimum requirement in the 1971 ACI Building Code[2] for vertical web reinforcement.

In Phase 5, the behavior of Specimens B7-5 and B8-5 were compared with that of Specimen B3-2, to determine the effect of height-to-horizontal length ratio. Both B7-5 and B8-5 had the same reinforcement percentages as B3-2. Their height-to-horizontal length ratios were 1/4 and 1, respectively.

Representation of Seismic Loading

The application of load reversals was intended to represent forces that would occur during a severe earthquake. To make it possible to compare the behavior of the specimens, a systematic pattern of increasing force or deflection was followed, as illustrated in Fig. 4.

At load stages prior to maximum, force was applied in increasing levels, as shown in Fig. 4. At each level, the load was cycled twice. Increments in load levels equivalent to a nominal shear stress of approximately $2\sqrt{f'_c}$ psi were used.

A load stage corresponds to the period during the test when the deflection was held constant and data readings were taken. During the application of force to obtain a new higher level, a load stage was also included at the previous load level. This procedure was followed in both directions of loading.

In the stages after maximum, force was applied until a desired value of deflection was reached. At each deflection increment, the load was cycled twice, maintaining approximately equal deflections in both directions of loading. The deflection was then increased until a new maximum load was obtained. During the application of force to obtain a new higher deflection, a load stage was also included at the previous deflection. This procedure was followed in both directions of loading.

TEST RESULTS

Principal Results

Principal test results are summarized in Table 5. Included are the nominal shear stresses and deflections

at first shear cracking and at ultimate load. The nominal shear stress at the end of the test is also listed.

Shear stress, v, was calculated from the following relationship:

$$v = \frac{V}{hd} \qquad (1)$$

where

V = shear force
h = overall thickness of the web
d = distance from extreme compression fiber to the centroid of the tension reinforcement

Calculations of the effective depth, d, are based on the assumption that strains in the reinforcement and concrete are directly proportional to the distance from the neutral axis. Both vertical web reinforcement and flange reinforcement were considered in these calculations.

As listed in Table 1, the lowest value of d is 67.8 in. (1.72 m) for B1-1, the specimen with the least amount of flexural flange reinforcement. The highest value of d is 73.0 in. (1.82 m) for B5-4, a specimen with no vertical web reinforcement.

In most specimens, the first observed cracking occurred in the lower portion of the web near the flange closest to the applied load. Usually, one or two very short cracks inclined at about 40 degrees were found. This cracking occurred at nominal shear stresses between 110 and 230 psi (7.7 and 16.2 kg. per sq. cm). It may have been influenced by residual tensile stresses in the web. Development of the first observed cracks did not noticeably affect the measured load-deflection relationships and the reinforcement load-strain relationships of the specimens.

At a higher stress, one or more long inclined cracks occurred suddenly in a location away from the other cracks. Development of long cracks usually coincided with a change in slope in the load-deflection and load-strain relationships. The occurrence of this cracking is referred to as first shear cracking.

Table 5 lists the nominal shear stress at first shear cracking, v_{cr}, and the corresponding deflection, $\Delta\ell$. Except for B3-2R, which was repaired, specimens with an h_w/ℓ_w of 1/2 had a narrow range of $v_{cr}/\sqrt{f'_c}$,

varying from 4.9 to 6.5.

To obtain a comparison of $\Delta\ell$ at first shear cracking between specimens of different heights, the value of $\Delta\ell/h_w$ is also listed in Table 5. This value ranged from 0.00032 for B5-4 and B7-5, to 0.00072 for B1.1.

Equation (11-32) in Section 11.16 of the 1971 ACI Building Code[2] is based on the assumption that web-cracking occurs when the principal tensile stress at the centroidal axis of the cross section reaches approximately $4\sqrt{f'_c}$. The calculated nominal shear stress, v, corresponding to a centroidal principal stress of $4\sqrt{f'_c}$ a transformed cross section, including all vertical reinforcement, was found to range from $3.4\sqrt{f'_c}$ for B5-4 to $3.8\sqrt{f'_c}$ for B2-1. Except for repaired Specimen B3-2R, these values were all lower than the measured values of $v_{cr}/\sqrt{f'_c}$ as reported in Table 5. Although the assumed critical principal tensile stress of $4\sqrt{f'_c}$ is a conservative lower bound, a higher value would appear justified by these results.

Table 5 also lists the nominal shear stress at ultimate, v_u, and the corresponding deflection, $\Delta\ell$. The value of $v_u/\sqrt{f'_c}$ ranged from 8.3 to 15.8, and the value of $\Delta\ell/h_w$ from 0.0053 to 0.0130. For the specimens with h_w/ℓ_w of 1/2, except for Specimen B3-2R, $\Delta\ell_w/h_w$ had a quite narrow range, from 0.0053 to 0.0069.

In Figure 5 the effect of the principal variables on v_c and v_u are shown. Figure 5 (a) shows the relationship between the amount of flange reinforcement, and the method of loading for three specimens that contained 0.5% horizontal and vertical wall reinforcement. The height-to-horizontal length ratio of each of the three walls was 1/2. In comparing the two specimens subjected to loading in one direction, it can be seen that the amount of flange reinforcement had little effect on the shear strength. The specimen subjected to load reversals, simulating seismic loading, exhibited a shear strength about 10% lower than that of specimens subjected to loading in one direction.

The effect of the amount of horizontal wall reinforcement is shown in Figure 5 (b). The two specimens

compared contained 4.1% reinforcement in the flanges and 0.5% vertical wall reinforcement. Their height-to-horizontal length ratio was 1/2. As can be seen, the amount of horizontal wall reinforcement had little effect on the shear strength.

Figure 5 (c) shows the effect of the vertical wall reinforcement. The three specimens compared contained 4.1% reinforcement in the flanges, and 0.5% horizontal reinforcement in the wall. The height-to-horizontal length ratio of each wall was 1/2. It can be seen that the shear strength increased significantly with added vertical wall reinforcement.

The effect of the height-to-horizontal length ratio is shown in Figure 5 (d). All three specimens compared contained 4.1% reinforcement in the flanges. In the wall, 0.5% vertical and horizontal reinforcement was used. Figure 5 (d) shows that for the specimen with the largest h_w/ℓ_w, both v_u and v_{cr} were lower than for the specimens with smaller h_w/ℓ_w.

Except for the specimen with an h_w/ℓ_w of 1, v_{cr} was not significantly affected by the different variables. The values of v_u and v_c calculated in accordance with Section 11.16 of the 1971 ACI Building Code[2] were always lower than the measured values of v_u and v_{cr}, respectively.

The tests were concluded after pushing the specimens to a maximum deflection of about 3 in. The corresponding values of nominal shear stress, v_m, and $v_m/\sqrt{f'_c}$ are listed in Table 5. The value of $v_m/\sqrt{f'_c}$ ranged from 2.6 to 5.7. The tallest specimen, B8-5, had the smallest $v_m/\sqrt{f'_c}$. For the specimens with h_w/ℓ_w of 1/2, $v_m/\sqrt{f'_c}$ ranged from 3.0 to 5.5.

Description of Behavior

Behavior of each specimen is summarized in Figure 6. The bar chart for a specimen notes the following stages corresponding to the numbers on the chart:

1. First observed crack
2. First shear crack
3. First yield of a vertical wall bar
4. First yield of a horizontal wall bar

Cracking resulting from loading both from the left and from the right of the specimens are shown.

Except for Specimen B7-5 first cracking occurred in the lower corner of the wall nearest the applied loads. These small inclined cracks occurred prior to any visible cracking in the flanges. For B7-5, the shortest specimen, the first cracking occurred in the central part of the wall.

In B1-1, several flexural cracks developed in the flange soon after first cracking in the wall was observed. These flexural cracks were distributed from the base up to the intersection of the flange with the first observed inclined cracks. As the load was subsequently increased, the next adjacent inclined shear cracks developed in the central region of the web. This was followed by further cracking in the flange.

In all other specimens, first shear cracking occurred suddenly in the wall before any significant flexural cracking was observed in the flanges. However, flexural cracking was observed either immediately afterwards, at the same load, or shortly thereafter at a load slightly higher than that corresponding to first shear cracking.

Yielding of the web reinforcement was generally observed to occur when the inclined cracking was at an advanced stage of development. In B3-2, the horizontal wall reinforcement was not observed to yield until after the ultimate load was reached.

Photographs showing the cracking in all of the specimens at ultimate load and after being subjected to additional load cycles that cause complete destruction are shown in Figure 7 and 8, respectively.

There was substantial cracking in the upper fibers of the top slab during the test. Also, upward movement of the central portion of the top slab was observed during later stages of loading.

Deflections

The measured deflections of Specimens B1-1 and B2-1 are shown in Figure 9. Load on Specimen B1-1 was rapidly released after ultimate was attained. The load versus deflection relationship for B1-1 would probably have been similar to that of B2-1 if this rapid unloading had not occurred.

Representative load versus deflection curves for B3-2, prior to and after ultimate, are shown in Figure 10. These curves reflect three modes of response represent-

ative of all specimens subject to load reversals. Near zero deflection, the curves have a shallow slope, attributed to observed slippage at joint and inclined crack interfaces. As deflection increases, the curves are linear and have maximum slope. This corresponds to the composite functioning of concrete and reinforcement. Finally, as the load or deflection is further increased, the response is non-linear. In this region, the specimen usually developed new or extended cracking as well as joint slippage between the wall and top slab.

The deflection curves in Figure 10 illustrate the manner in which the deflection "envelope" was obtained for a specimen subject to load reversals. In Figure 9, the deflection envelope for B3-2 may be compared with the measured deflection of B1-1 and B2-1. Deflection envelopes for the remaining specimens that were subjected to cyclic loads are compared in Figures 11, 12, and 13.

Strain Distribution

As previously discussed, the test results indicated that vertical wall reinforcement was the most significant variable affecting the strength of the test specimens. Information on vertical strain at three levels - base, mid-height, and top of wall - are presented for B3-2, B7-5, and B8-5 in Figures 14, 15, and 16, respectively. Except at loads prior to cracking, these figures show clearly that the strain distribution in the specimens was non-linear and not indicative of beam behavior.

Except for B8-5, the measured strains in the horizontal wall reinforcement were generally less than in the vertical reinforcement. Averages of several horizontal and vertical wall reinforcement strains in the central part of these three specimens are plotted in Figure 17. In B8-5, the vertical and horizontal strains are approximately equal.

Repair and Re-test of B3-2

To determine the effectiveness of repairs of a shear wall after it has been severely damaged, B3-2 was repaired, designated as B3-2R, and re-tested. At the end of the test on B3-2, as shown in Fig. 8, the top of the wall had a residual deflection of about 2 in. The hydraulic rams were used to push the top of the specimen back to its non-deflected position.

Damaged cracked concrete was removed from the wall with an electric hammer and a chisel. All surfaces were cleaned by washing with water. The only sound concrete left after removal was a portion that extended up from the base approximately 8 in.

Plywood was used to form the sides of the wall. Prior to placing the concrete, two-component, epoxy-polysulfide resin was applied to the joint between the web and the top slab. This resin is used to bond freshly mixed plastic concrete or mortar to hardened concrete or other structural materials.

Concrete was placed through a slot at the top of one of the panels, and was hand packed against the underside of the top slab. After packing, the top of the web was approximately 1/2-in. (12.7 mm) thicker than other portions for a distance of about 1-in. (25.4 mm) beneath the top slab. At test, the average compressive strength of the new wall concrete was 3410 psi (240 kg per sq.cm).

After stripping, it was estimated that there was a visible gap in about 5% of the horizontal length between the recast wall and top slab. This gap was patched with a cement mortar mix.

The loading used was the same as described in Fig. 4 with the exception that at each level, the load was cycled only once. Figure 18 shows the envelope of all the load versus deflection curves for B3-2R. For comparison, the envelope for B3-2 is also shown.

During the test on B3-2R, a short inclined crack in the lower left portion of the wall and first shear cracking in the central region of the web both occurred at a nominal shear stress, v_{cr}, of 190 psi (13.4 kg per sq. cm). First cracking was observed in the flanges at a nominal shear stress of 260 psi (18.3 kg per sq. cm).

By the time the maximum load was reached, inclined cracking was distributed over the entire web in both directions. The majority of these cracks were at an angle of about 40 degrees. At maximum load, slipping and spalling developed along the junction of the top slab and the wall. This was followed by crushing in the upper part of the wall near the left flange.

The shear strength, v_u, of Specimen B3-2R was 680 psi (47.8 kg per sq. cm) in one direction. Subsequently, the maximum nominal shear stress due to loading in the other direction was 595 psi (41.8 kg per sq. cm). Figure 19 shows B3-2R at the ultimate load.

As shown in Figure 18, B3-2R exhibited a gradual decrease in load-carrying capacity after maximum load was reached. Beyond 1-1/2-in. (38 mm) lateral displacement, no reduction in capacity was observed.

As the load was being applied beyond ultimate, slip was clearly visible at the junction of the wall and the top slab. This slip was accompanied by the concrete being pushed out by the vertical bars along the mid-horizontal length of the wall. The wall concrete near the junction with the flange was completely destroyed.

When a total lateral displacement of approximately 3-in. (76.2 mm) was reached, the nominal shear stress, v_m, was 230 psi (16.2 kg per sq. cm). Finally, the specimen was unloaded and a recovery of 1.2-in. (30.5 mm) deflection was observed. Figure 20 shows B3-2R after the re-test was concluded.

The shear strength of 680 psi (47.8 kg per sq. cm) for B3-2R was 23% lower than the 880 psi (61.9 kg per sq. cm) measured for B3-2. However, the value of $v_u/\sqrt{f'_c}$ for the repaired specimen was 11.5. This is greater than the maximum of 10 permitted by Section 11.16 of the 1971 ACI Building Code[2].

ANALYSIS

Shear Cracking

In the previous description of behavior, it was noted that the first observed cracking usually occurred in the lower corners of the wall. These relatively short inclined cracks probably occurred because of residual shrinkage stresses in the corners of the wall. Since they gave no indication of influencing the behavior of the specimens, this early cracking was not considered to be significant.

Shear cracking usually occurred suddenly, when one or more long inclined cracks developed in the wall. It is believed that cracks frequently observed to occur at the same time in the flanges formed as a result of the shear cracking. Therefore, the development of shear cracking should be related to stresses in the web exceeding the tensile strength of the concrete.

Values of the principal tensile stress, f_{pt}, were computed from the relationship $f_{pt} = VQ/Ih$, where V was the applied load at v_{cr}, Q and I are properties of the cross section computed using a transformed uncracked section, and h=4 in.(120 mm), the thickness of the wall. Expressed in terms of the concrete strength of

each specimen, f_{pt} ranged from $5.5\sqrt{f'_c}$ psi for B2-1 to $7.1\sqrt{f'_c}$ psi for B1-1, except for B8-5 with a computed value of $3.9\sqrt{f'_c}$ psi. The value of f_{pt} for B7-5 was $6.1\sqrt{f'_c}$ psi.

Equation (11-32) of the ACI Building Code[2] is based on the assumption that the shear carried by the concrete, v_c, is equal to that at shear cracking, and that shear cracking occurs when $f_{pt} = 4\sqrt{f'_c}$ psi ($1.06\sqrt{f'_c}$ kg per sq. cm). It is therefore evident that Equation (11-32) would have underestimated the stress at shear cracking in all test specimens, even when subjected to load reversals. In fact, these test results suggest that taking $f_{pt} = 6\sqrt{f'_c}$ would be appropriate for the specimens with height to length ratio equal to or less than one-half.

Ultimate Load

Whether the load was applied to the specimens in one direction or with reversals, the shear appeared to be transferred from the top slab to the base by a lattice system. This system consisted of the vertical wall and flange reinforcement acting in tension and the concrete struts in the wall between inclined cracks acting in compression. Verification of this analogy was obtained by an indirect computation of the magnitude and location of the resultant compressive force at the base, mid-height, and top of the wall. First, the resultant tensile force was computed from measured strains in the vertical reinforcement in the wall and flanges. Measured strains in the flange reinforcement on the opposite side of the applied load were generally small, and as often in tension as in compression. The location of the resultant compressive force, assuming it to be equal to the tensile force, was determined by assuming it to be in equalibrium with the known applied load.

A plot of the computed locations of the compressive thrust for the specimens with $h_w/\ell_w = 0.5$ is shown in Figure 21. It may be seen that these locations are in a sloping band that closely corresponds to the observed inclination of the shear cracks. For comparison, the cross hatched band includes the locations of the compressive thrust if the usual assumptions for beam behavior are applied.

Even though the lattice analogy provided good conceptual agreement with the observed behavior, it was

found that the shear computed as the product of the measured compressive thrust times the tangent of the crack inclination, taken equal to 38°, was in only fair agreement with the applied shear. Ratios of the computed shear to the applied shear, for test specimens with $h_w/\ell_w = 0.5$, ranged from 1.06 to 1.76. However, if B2-1 and B4-3 are excluded, the ratios ranged from 1.06 to 1.33.

The test program was arranged to permit a direct evaluation of shear strength which conforms to the current design practice of assuming

$$v_u = v_c + v_s$$

where v_c and v_s are the contribution to shear strength provided by the concrete and by the shear reinforcement, respectively. As may be seen from Table 5, comparison of the strength of B4-3 with B3-2 shows that the horizontal wall reinforcement was not effective. However, comparison of B5-4 and B6-4 with B3-2 clearly indicates that the vertical shear reinforcement was highly effective. Assuming, then, that the horizontal shear reinforcement in B5-4 was not effective, the strength without vertical or horizontal shear reinforcement is approximately $v_c = 8.3\sqrt{f'_c}$ psi.

The increase in strength obtained with the addition of vertical wall reinforcement is plotted in Figure 22. Since the contribution of v_s is assumed in design to be independent of concrete strength, the values of v_s in Figure 22 are taken equal to $v_u - 8.3\sqrt{f'_c}$ psi. The solid line fitted to the test points indicates that the contribution of v_s is directly related to $\rho_n f_y$. The strength of these specimens is, therefore, adequately represented by $v_u = 8.3\sqrt{f'_c} + \rho_n f_y$.

The test results for B7-5 and B8-5, as shown in Figure 5 (d), indicate that h_w/ℓ_w has an influence on shear strength. However, since the difference between v_u and v_{cr} is nearly constant, the differences in strength appear due largely to differences in v_c. It was noted that joint distress was observed in the test on B7-5. Therefore somewhat greater reliance is placed on the difference in strength observed between B3-2 and B8-5, indicating that v_c may be taken equal to $8.3\sqrt{f'_c}$ -

$3.4\sqrt{f'_c}\left(\frac{h_w}{\ell_w} - \frac{1}{2}\right)$.

The following equation provides a close prediction of the shear strength of the test specimens and reflects the variables found to be significant:

$$v_u = 8.3\sqrt{f'_c} - 3.4\sqrt{f'_c}\left(\frac{h_w}{\ell_w} - \frac{1}{2}\right) + \rho_n f_y \text{ in psi}$$

This equation is expected to be applicable to walls similar to the test specimens within the following ranges:

$$2500 \text{ psi} \leq f'_c \leq 4500 \text{ psi}$$

$$(176.0 \text{ kg. per sq. cm} \leq f'_c \leq 316.0 \text{ kg. per sq. cm})$$

$$0 \leq \frac{h_w}{\ell_w} \leq 1$$

$$0.25\% \leq \rho_n \leq 0.5\% \text{ and somewhat higher}$$

$$\rho_h \geq 0.25\%$$

Post-Ultimate Load Behavior

Beyond ultimate load, gradual cracking and spalling of the concrete in the wall occurred as the specimens were subjected to continually increasing reversed deflections. As the wall was further damaged, shear resistance was transferred from the wall to the flange boundary elements. As can be seen from Figure 23 (a), the lateral load is finally resisted by frame action of the flanges and top slab. However, the part of the web that remains offers substantial restraint to lateral movement of the flanges.

An idealization of the observed frame action is shown in Figure 23 (b). The maximum shear that can be applied to this frame may be expressed in terms of the moment capacity of the flanges, M_{uf}, as follows:

$$v_m = \frac{4M_{uf}}{h_{we}hd}$$

Using values of M_{uf} computed in accord with Section 10.2 of the 1971 Building Code [2] and based on measured material properties, and assuming $h_{we} = 1/3\ \ell_w$ when $h_w/\ell_w = 1$, $1/2\ \ell_w$ when $h_w/\ell_w = 1/2$, and $7/12\ \ell_w$ when $h_w/\ell_w = 1/4$, v_m is equal to 183, 167, 179, 300, and 142 psi for B3-2, B4-3, B6-4, B7-5, and B8-5, respectively (100 psi=

7.03 kg. per sq. cm). The ratios of the measured values of v_m at the end of the test, given in Table 5, with the computed values for these specimens are 1.04, 0.96, 1.06, 1.02, and 1.06, respectively.

Comparisons are not made for the other three test specimens because B1-1 and B2-1 were not subjected to load reversals. Also, the behavior of B5-4 differed from that of others due to the absence of vertical wall reinforcement.

Comparisons with Provisions in ACI 318-71

In Figure 5, the test results are compared with values predicted by Section 11.16, "Special Provisions For Walls," of the 1971 ACI Building Code[2]. It is noted that minimum requirements for ρ_h and ρ_n preclude comparisons with some of the specimens.

For the computation of v_c, Equation (11-32) gave a value lower than that obtained from Equation (11-33) since the maximum value of M_u/V_u in the latter equation for any of the test specimens is $\ell_w/2$ for B8-5. Since $N_u = 0$, Equation (11-32) indicates that $v_c = 3.3\sqrt{f'_c}$ psi. As may be seen from Figure 5, the observed values of v_{cr} are all substantially greater than v_c except for B8-5, the specimen with $h_w/\ell_w = 1$, where v_c and v_{cr} are nearly equal.

The contribution of the horizontal reinforcement, determined from Equation (11-13), may be expressed as $v_s = v_u - v_c = \rho_h f_y$. Taking average values of f_y equal to 72.4 ksi (5089 kg. per sq. cm) and f'_c equal to 3450 psi (242.5 kg. per sq. cm), $v_u = 6.4\sqrt{f'_c}$ psi for $\rho_h = 0.25\%$ and $9.5\sqrt{f'_c}$ psi for $\rho_h = 0.5\%$. Where comparisons can be made, as indicated by the dashed lines in Figure 5, it is evident that the measured values are substantially in excess of those calculated. It is also significant that the maximum measured values of v_u are as much as 50% greater than the limiting value of $v_u = 10\sqrt{f'_c}$ psi specified in Section 11.16.5.

The test results may also be compared with values predicted by Section 11.9, "Special Provisions for Deep Beams," and by Section 11.15, "Shear-Friction." The

provisions for deep beams are limited to members loaded directly on the extreme compressive fibers. This restriction implies that the shear carried by the concrete, v_c, may be taken greater than v_{cr}, the value of shear stress causing diagonal tension cracking. The evaluation of shear strength of the test specimens clearly indicated that for these specimens, v_c was greater than v_{cr}.

For deep beams, the value of v_c is computed from Equation (11-22). However, v_c is limited to $6\sqrt{f'_c}$ psi for all of the test specimens. The contribution of the shear reinforcement is determined from Equation (11-24) and may be expressed as

$$v_s = v_u - v_c = \rho_h f_y \left(\frac{1 + \frac{2h_w}{d}}{12}\right) + \rho_n f_y \left(\frac{11 - \frac{2h_w}{d}}{12}\right)$$

For B3-2, h_w/d was 0.53. Therefore, $v_u = 6\sqrt{f'_c} + 0.17 \rho_h f_y + 0.83 \rho_n f_y$. Evaluating the latter two terms and expressing v_s in terms of the concrete strength in B3-2, $v_u = 12.2\sqrt{f'_c}$ psi. Although this value exceeds the limit of $8\sqrt{f'_c}$ psi allowed by Section 11.9.4, the computed value of $12.2\sqrt{f'_c}$ psi is in reasonable agreement with the measured value of $14.1\sqrt{f'_c}$ psi.

Similarly for B7-5, $\frac{h_w}{d}$ was 0.26 and $v_u = 6\sqrt{f'_c} + 0.13 \rho_h f_y + 0.87 \rho_n f_y = 12.2\sqrt{f'_c}$ psi. For this specimen, the measured value was $14.8\sqrt{f'_c}$ psi. For B8-5, h_w/d was 1.06 and $v_u = 6\sqrt{f'_c} + 0.26\rho_h f_y + 0.74\rho_n f_y = 12.4\sqrt{f'_c}$ psi. This is in good agreement with the measured value of $12.1\sqrt{f'_c}$ psi. These comparisons indicate that the deep beam provisions provide a reasonable prediction of the strength of the test specimens if the upper limit on v_u is disregarded.

The provisions for shear-friction apply when it is inappropriate to consider shear as a measure of diagonal tension. They may, therefore, be used to provide an estimate of the shear strength of the joint between the wall and the top slab.

They also may be considered to provide an estimate of shear capacity of the specimen.

While it is difficult to assess the distribution of shear in the joint between the flanges and the wall, it is common practice to assume that most of the shear is resisted by the wall. Applying Equation (11-30), the ultimate shear may be expressed as

$$V_u = A_{vf} f_y \mu = \rho_n f_y \mu b_w (\ell_w - 8)$$

Therefore the nominal ultimate shear stress is

$$v_u = \rho_n f_y \mu \frac{(\ell_w - 8)}{d}$$

Taking $(\ell_w - 8)/d = 0.95$ for the test specimens, and taking $\mu = 1.0$ and f_y equal to the average value of 77.3 ksi (5730 kg. per sq. cm), v_u = 184 psi (12.9 kg. per sq.cm) for $\rho_n = 0.25$ and 367 psi (25.8 kg. per sq. cm) for $\rho_n = 0.50\%$. Compared to the values of measured shear stress, given in Table 5, it is evident that these stresses are very conservative.

Design Suggestions

The observed strength of the test specimens was substantially greater than that expected from the provisions of Section 11.16 of the 1971 ACI Building Code[2]. Perhaps the most important finding is that previous concern over the applicability of Equation (11-32) to walls subjected to load reversals is clearly unfounded. Based on the results of the tests reported in this paper, it is suggested that the following expression be substituted for Equation (11-32):

$$v_c = 8\sqrt{f'_c} - 2.5\sqrt{f'_c}\,\frac{h_w}{\ell_w} + \frac{N_u}{4\ell_w h} \quad \text{in psi}$$

The first two terms of this equation are approximately 80% of the expression for v_c determined to best represent the tests in this investigation.

While Section 11.16.4 places emphasis on the value of the horizontal shear reinforcement, the provision requires that ρ_n be at least equal to ρ_h for walls with h_w/ℓ_w of less than one. Therefore, the provision will give conservative requirements for shear reinforcement.

Figure 24 shows the relationship between observed stress at maximum load, v_u (test), and calculated ultimate stress, v_u (calc). The comparison indicates that the results of tests in this investigation are in reasonable agreement with those predicted.

ACKNOWLEDGMENTS

This paper is based on an experimental investigation carried out by Dr. Felix Barda under the supervision of the other authors at the Structural Laboratory of the Portland Cement Association. The research was the basis for Dr. Barda's thesis[22] at Lehigh University. Dr. D. A. VanHorn was the professor in charge of Dr. Barda's program.

The capable assistance of the technicians and clerical staff of the Association, including B. W. Fullhart, O. A. Kurvits, W. Hummerich, and B. Doepp is gratefully acknowledged.

REFERENCES

1. ACI Committee 318, "Building Code Requirements for Reinforced Concrete (ACI 318-63)," American Concrete Institute, Detroit, Michigan, June 1963, 144 pp.

2. ACI Committee 318, "Building Code Requirement for Reinforced Concrete (ACI 318-71),"American Concrete Institute, Detroit, Michigan, February 1971, 78 pp.

3. ACI-ASCE Committee 326 (426), "Shear and Diagonal Tension," ACI Journal, Proceedings, Vol. 59, No. 1 January 1962, pp. 1-30, No. 2 February 1962, pp. 277-334; and No. 3 March 1963, pp. 352-396.

4. MacGregor, J. G. and Hanson, J. M., "Proposed Changes in Shear Provisions for Reinforced and Prestressed Concrete Beams," ACI Journal, Proceedings, Vol. 66, April 1969, pp. 276-288.

5. MacGregor, James G., Chairman, et al, "The Shear Strength of Reinforced Concrete Members," by the Joint ASCE-ACI Task Committee on Masonry and Reinforced Concrete of the Structural Division, Journal of the Structural Division, ASCE, Vol. 99, No. ST6, Proc. Paper 9791, June 1973, pp. 1091-1187.

6. Austin, W. J., Untrauer, R. E., Egger, W., Winemiller, J. R., "An Investigation of the Behavior of Deep Members of Reinforced Concrete and Steel," Structural

Research Series No. 187, Civil Engineering Studies, University of Illinois, January 1960.

7. de Paiva, H. A. R., and Austin, W. J., "Behavior and Design of Deep Structural Members; Part 3: Tests of Reinforced Concrete Deep Beams," Structural Research Series No. 194, Civil Engineering Studies, University of Illinois, March 1960.

8. Winemiller, J. R., and Austin, W. J., "Behavior and Design of Deep Structural Members, Part 2: Tests of Reinforced Concrete Deep Beams with Web and Compression Reinforcement," Structural Research Series No. 193, Civil Engineering Studies, University of Illinois, August 1960.

9. de Paiva, H. A. R., "Strength and Behavior in Shear of Reinforced Concrete Deep Beams Under Static and Dynamic Loading," Ph.D. Dissertation, University of Illinois, Urbana, Illinois, 1961.

10. Franz, G., and Niendenhoff, H., "The Reinforcement of Brackets and Short Deep Beams," Beton and Stahlbetonbau, Vol. 58, No. 5, (Translation No. 114, Cement and Concrete Association, London, England, December 1964), May 1963.

11. Leonhardt, F., and Walther, R., "Wandartige Trager," Deutscher Ausschuss fur Stahlbeton, Technische Hochschule, Stutgart, West Germany, 1966.

12. Crist, Robert A., "Shear Behavior of Deep Reinforced Concrete Beams, V. II, Static Tests," Technical Report No. AFWL-TR-67-61, Kirtland Air Force Base, New Mexico, October 1967.

13. Williams, H. A., Benjamin, J. R., "Investigation of Shear Walls, Part 3 - Experimental and Mathematical Studies of the Behavior of Plain and Reinforced Concrete Walled Bents Under Static Shear Loading," Department of Civil Engineering, Stanford University, July 1, 1953.

14. Benjamin, Jack R., Williams, H. A., "Investigation of Shear Walls, Part 6 - Continued Experimental and Mathematical Studies of Reinforced Concrete Walled Bents Under Static Shear Loading," Department of Civil Engineering, Stanford University, August 1, 1954.

15. Benjamin, Jack R., Williams, Harry A., "Investigation of Shear Walls, Part 9 - Continued Experimental and Mathematical Studies of Reinforced Con-

crete Walled Bents Under Static Shear Loading," Department of Civil Engineering, Stanford University, September 1, 1955.

16. Benjamin, Jack R., Williams, Harry A., "Investigation of Shear Walls, Part 12 - Studies of Reinforced Concrete Shear Walls Assemblies," Department of Civil Engineering, Stanford University, December 1956.

17. Stivers, R. H., Benjamin, J. R., and Williams, H. A., "Investigation of Shear Walls, Part 8 - Stresses and Deflections in Reinforced Concrete Shear Walls Containing Rectangular Openings," Department of Civil Engineering, Stanford University, August 1954.

18. Antebi, J., Utku, S., and Hansen, R. J., "The Response of Shear Walls to Dynamic Loads," MIT Department of Civil and Sanitary Engineering, Cambridge, Massachusetts, August 1960.

19. Galletly, G. D., "Behavior of Reinforced Concrete Shear Walls Under Static Load," MIT Department of Civil and Sanitary Engineering, Cambridge, Massachusetts, August 1952.

20. Cardenas, A. E., Hanson, J. M., Corley, W. G., and Hognestad, E., "Design Provisions for Shear Walls," ACI Journal, Proceedings, Vol. 70, March 1973, pp. 221-230.

21. Cardenas, A. E., and Magura, D. D., "Strength of High-Rise Shear Walls - Rectangular Cross Sections," Response of Multistory Concrete Structures to Lateral Forces, American Concrete Institute Publication SP-36, Detroit, Michigan, 1973, pp. 119-150.

22. Barda, F., "Shear Strength of Low-Rise Walls with Boundary Elements," Ph.D. Thesis, Lehigh University, Bethlehem, Pennsylvania, 1972.

23. Hognestad, E., Hanson, N. W., Kriz, L. B., and Kurvits, O. A., "Facilities and Test Methods of PCA Structural Laboratory," papers under various titles in Journal of the PCA Research and Development Laboratories, V. 1 No. 1, January 1959, pp. 12-20, 40-44; V. 1, No. 2, May 1959, pp. 30-37; and V. 1, No. 3, September 1959, pp. 35-41; reprinted jointly as PCA Development Department Bulletin D33.

24. Hanson, N. W., Hsu, T. T. C., Kurvits, O. A. and Mattock, A. H., "Facilities and Test Methods of PCA Structural Laboratory -- Improvements 1960-65," papers under various titles in Journal of the PCA Research and Development Laboratories, V. 3, No. 2, May 1960, pp. 27-31; V. 7, No. 1, January 1965, pp. 2-9; and V. 7, No. 2, May 1965, pp. 24-38; reprinted jointly as PCA Development Department Bulletin D91.

NOTATION

A_{vf} = area of shear-friction reinforcement.

d = distance from extreme compressive fiber to centroid of tension reinforcement.

E_c = modulus of elasticity of concrete.

f_s = allowable stress in steel.

f_{pt} = principal tensile stress.

f_u = tensile strength of steel.

f_y = yield stress of steel.

f'_c = compressive strength of concrete.

$\sqrt{f'_c}$ = square root of the compressive strength of concrete, expressed in psi.

h = overall thickness of wall.

h_w = height of wall from base to center of top slab.

h_{we} = effective height of flanges.

I = moment of inertia.

ℓ_w = horizontal length of wall in inches.

M_u = ultimate moment.

M_{uf} = moment capacity of flange.

N_u = axial force normal to the cross section.

Q = statical moment of transformed area above or below the neutral axis.

v = nominal shear stress = V/hd.

v_c = nominal shear stress carried by the concrete section alone.

v_{cr} = nominal shear stress at first shear cracking.

v_m = nominal shear stress at end of test.

v_s = nominal shear stress carried by the web reinforcement.

v_u = nominal shear stress at ultimate load.

$v_u(calc)$ = calculated stress at ultimate load.

$v_u(test)$ = stress at measured ultimate load.

V_u = ultimate shear force.

V = shear force.

$\Delta\ell$ = deflection at the top of the specimen in the direction of loading.

μ = coefficient of friction.

ρ = ratio of area of reinforcement in flange to gross area of flange.

ρ_h = ratio of area of horizontal wall reinforcement to gross concrete area of the vertical section.

ρ_n = ratio of area of vertical wall reinforcement to gross concrete area of wall.

ϕ = reduction capacity factor.

TABLE 1 - DETAILS OF SPECIMENS

Specimen	Height h_w in.	$\frac{h_w}{\ell_w}$	Effective depth in.	Reinforcement					
				Flange		Wall Vertical		Wall Horizontal	
				No.-Size	Reinf. ratio ρ	No.-Size	Reinf. ratio ρ_n	No.-Size	Reinf. ratio ρ_h
B1-1	37.5	½	67.8	16-No.3	0.018	12-No.3	0.005	15 - 6mm	0.005
B2-1	37.5	½	71.7	20-No.5	0.064	12-No.3	0.005	15 - 6mm	0.005
B3-2	37.5	½	70.7	20-No.4	0.041	12-No.3	0.005	15 - 6mm	0.005
B4-3	37.5	½	70.6	20-No.4	0.041	12-No.3	0.005	None	0
B5-4	37.5	½	73.0	20-No.4	0.041	None	0	15 - 6mm	0.005
B6-4	37.5	½	71.8	20-No.4	0.041	16 - 6mm	0.0025	15 - 6mm	0.005
B7-5	18.75	¼	70.7	20-No.4	0.041	12-No.3	0.005	7 - 6mm	0.005
B8-5	75.0	1	70.7	20-No.4	0.041	12-No.3	0.005	33 - 6mm	0.005

Note: 1" = 25.4mm

TABLE 2 - CONCRETE PROPERTIES

Specimen	Base f'_c psi	Top Slab f'_c psi	Wall and Flanges: Age at test days	f'_c psi	f'_{sp} psi	$f'_{sp}/\sqrt{f'_c}$ psi	E_c[1] million psi
B1-1	4710	3810	35	4200	514	7.95	3.40
B2-1	3070	3090	29	2370	322	6.63	2.51
B3-2	3320	3720	27	3920	468	7.45	3.44
B3-2R[2]	-	-	7	3410	368	6.30	2.64
B4-3	5070	2660	29	2760	371	7.05	2.68
B5-4	4050	2890	28	4190	531	8.20	3.40
B6-4	4520	3350	27	3080	412	7.43	3.14
B7-5	4460	3760	26	3730	473	7.75	3.26
B8-5	4260	3320	26	3400	432	7.40	3.30
Average				3450			

[1] E_c = Measured secant modulus of elasticity for concrete

[2] Repaired Specimen B3-2

Note: 1000 psi = 70.3 kg/cm^2

TABLE 3 - REINFORCEMENT PROPERTIES

Specimen	Flanges						Wall			
	6mm Stirrups		D2 Cross-Ties		Vertical[1]		Vertical[4]		6mm Horizontal	
	Yield Stress f_y ksi	Ult. Stress f_u ksi	Yield Stress f_y ksi	Ult. Stress f_u ksi	Yield Stress f_y ksi	Ult. Stress f_u ksi	Yield Stress f_y ksi	Ult. Stress f_u ksi	Yield Stress f_y ksi	Ult. Stress f_u ksi
B1-1	72.5	97.4	60.0	63.5	76.2[2]	118.7[2]	78.8	123.1	71.9	98.6
B2-1	70.5	96.8	71.8	77.8	70.6[3]	119.0[3]	80.0	126.5	72.4	97.0
B3-2	70.0	96.3	69.8	77.0	60.0	96.7	79.0	123.3	74.4	97.5
B4-3	71.2	99.0	74.0	80.8	76.5	117.2	77.6	119.6	-	-
B5-4	68.7	96.7	71.9	-	76.4	117.0	-	-	71.8	98.3
B6-4	72.0	94.8	70.4	77.7	76.7	116.3	72.0[5]	94.8[5]	72.0	94.8
B7-5	72.7	96.0	66.2	71.2	78.2	115.1	77.0	120.4	72.7	96.0
B8-5	69.3	96.8	66.2	71.2	70.9	112.8	76.5	109.5	71.9	97.9

[1] No. 4 bars unless otherwise noted
[2] No. 3 bars
[3] No. 5 bars
[4] No. 3 bars unless otherwise noted
[5] 6mm bars

Note: 1 ksi = 70.3 kg/cm^2

TABLE 4 - TEST PROGRAM

Phase	Test Specimens Compared	Load Reversals	Purpose of Tests
1	B1-1, B2-1	No	Vary amount of main flexural reinforcement
2	B1-1, B2-1, B3-2	Yes	Assess reversals of loading
3	B3-2, B4-3	Yes	Vary amount of horizontal web reinforcement
4	B3-2, B5-4, B6-4	Yes	Vary amount of vertical web reinforcement
5	B3-2, B7-5, B8-5	Yes	Vary h_w/ℓ_w

TABLE 5 - PRINCIPAL TEST RESULTS

Specimen	Variable[1]	First Shear Cracking				Ultimate Load				End of Test	
		Shear Stress v_{cr} psi	$\frac{v_{cr}}{\sqrt{f'_c}}$	Defl $\Delta\ell$ in.	$\frac{\Delta\ell}{h_w}$	Shear Stress v_u psi	$\frac{v_u}{\sqrt{f'_c}}$	Defl $\Delta\ell$ in.	$\frac{\Delta\ell}{h_w}$	Shear Stress v_m psi	$\frac{v_m}{\sqrt{f'_c}}$
B1-1	ρ = 1.8%[2]	420	6.5	0.027	0.00072	1010	15.5	0.23	0.0061	280	4.4
B2-1	ρ = 6.4%[2]	240	4.9	0.016	0.00043	767	15.8	0.26	0.0069	270	5.5
B3-2	Control	330	5.2	not measured		881	14.1	0.21	0.0056	190	3.0
B3-2R	Repair	190	3.3	0.020	0.00053	676	11.5	0.49	0.0130	230	4.0
B4-3	ρ_h = 0	320	6.1	0.015	0.00040	810	15.4	0.20	0.0053	160	3.0
B5-4	ρ_n = 0	330	5.2	0.012	0.00032	538	8.3	0.20	0.0053	280	4.3
B6-4	ρ_n = 0.25%	280	5.0	0.013	0.00035	686	12.3	0.23	0.0061	190	3.5
B7-5	h_w/ℓ_w = 1/4	330	5.4	0.006	0.00032	906	14.8	0.16	0.0085	350	5.7
B8-5	h_w/ℓ_w = 1	200	3.5	0.027	0.00036	704	12.1	0.42	0.0056	150	2.6

Notes: [1]Except as indicated below all specimens had the following characteristics: h_w/ℓ_w = 1/2, ρ_h = 0.5%, ρ_n = 0.5%, ρ = 4.1%.

[2]Specimens subjected to static loading. All other specimens subjected to load reversals.

Note: 1 in. = 25.4mm, 1000 psi = 70.3 kg/cm^2

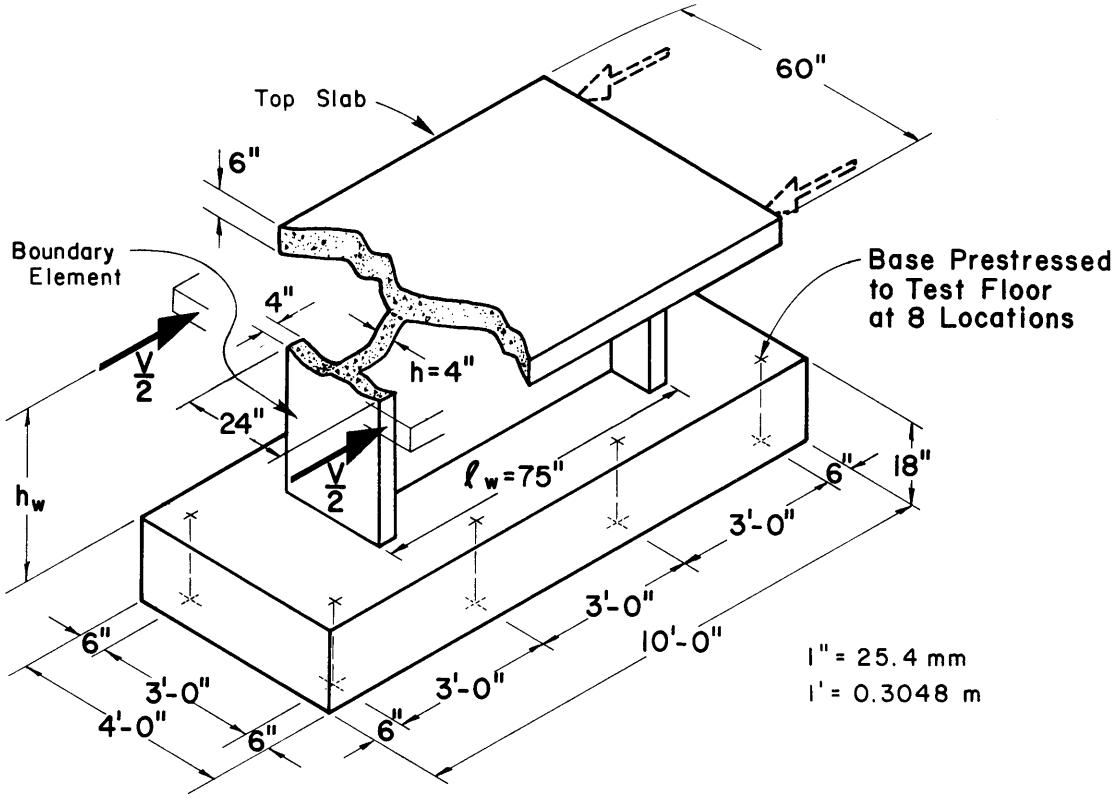

Fig. 1--Test specimen

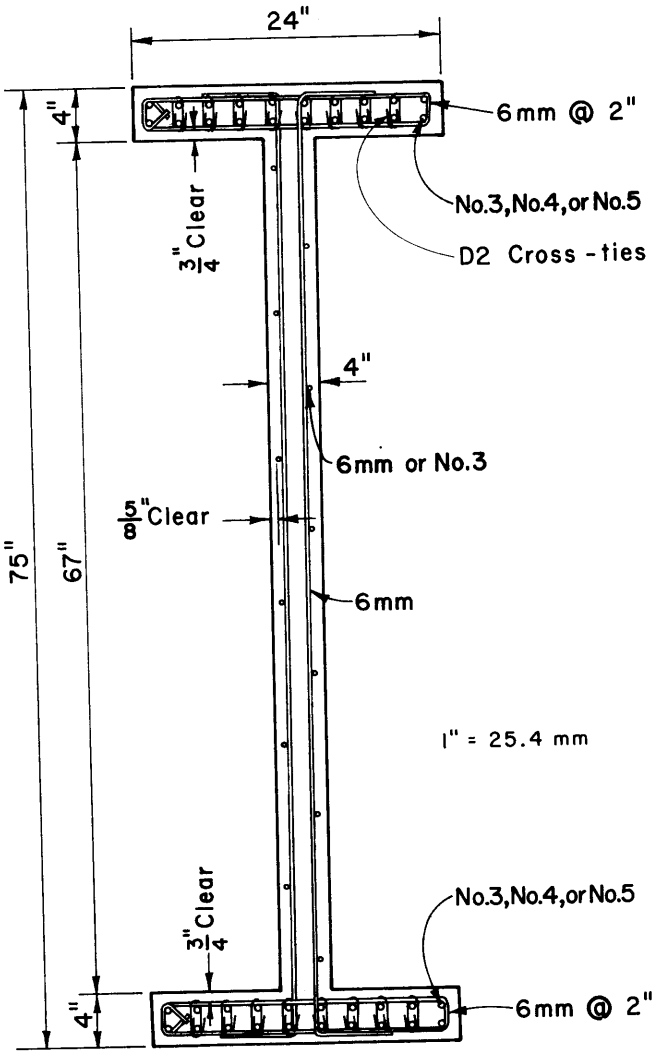

Fig. 2--Representative horizontal section

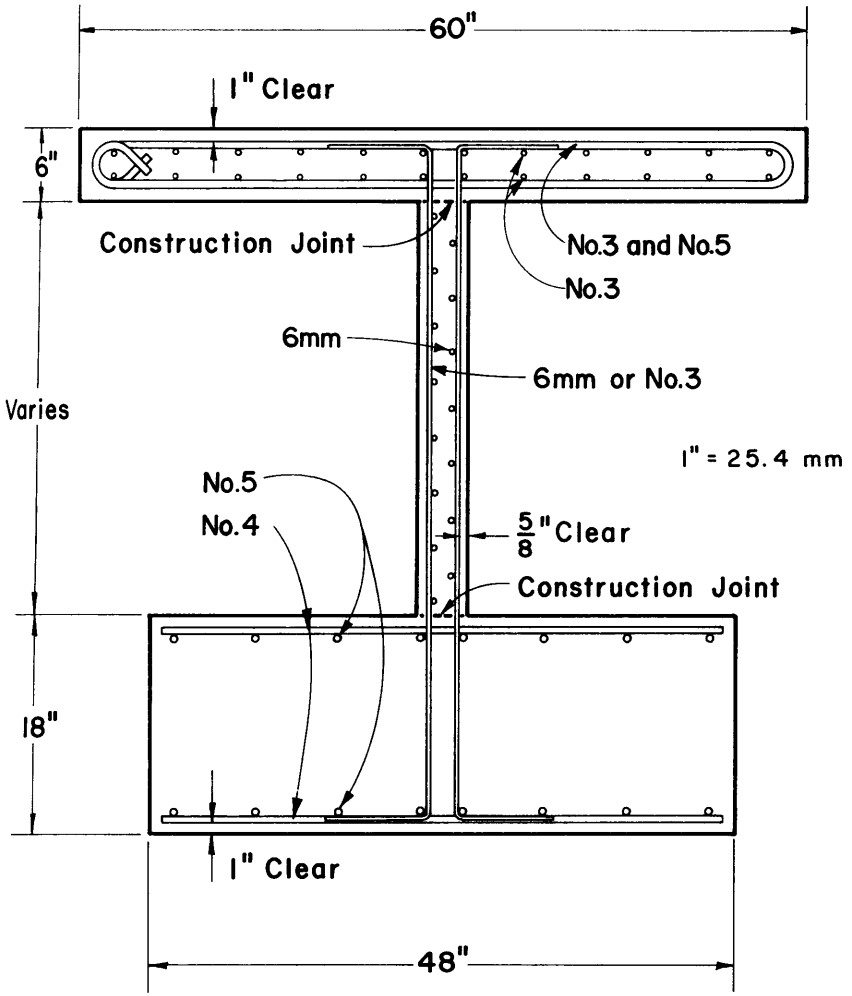

Fig. 3--Representative vertical section

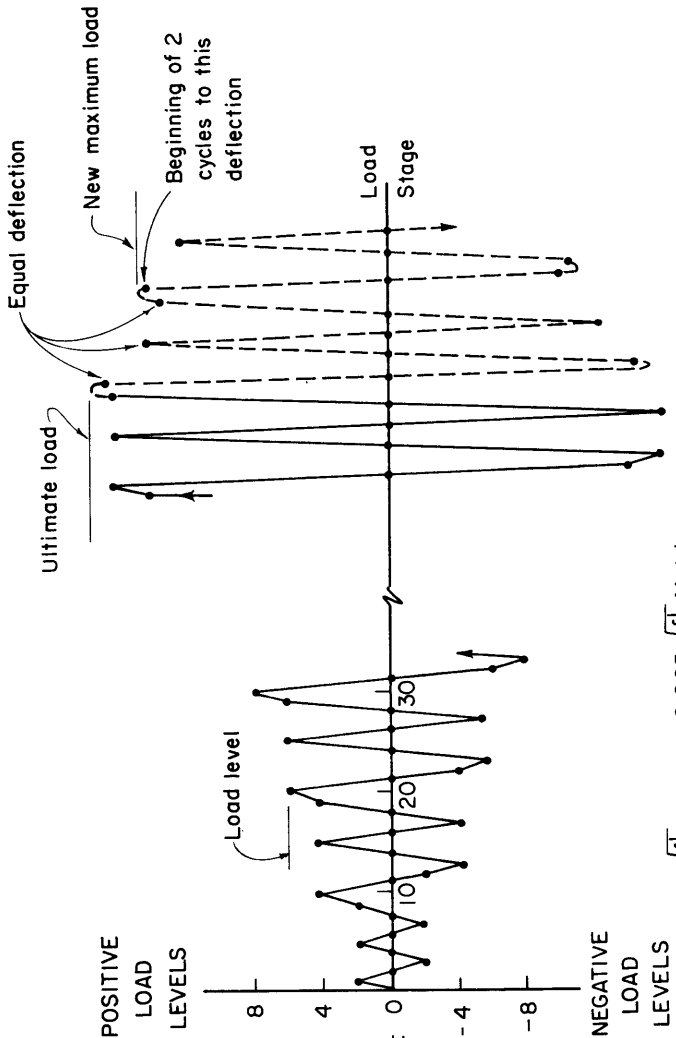

Fig. 4--Loading method

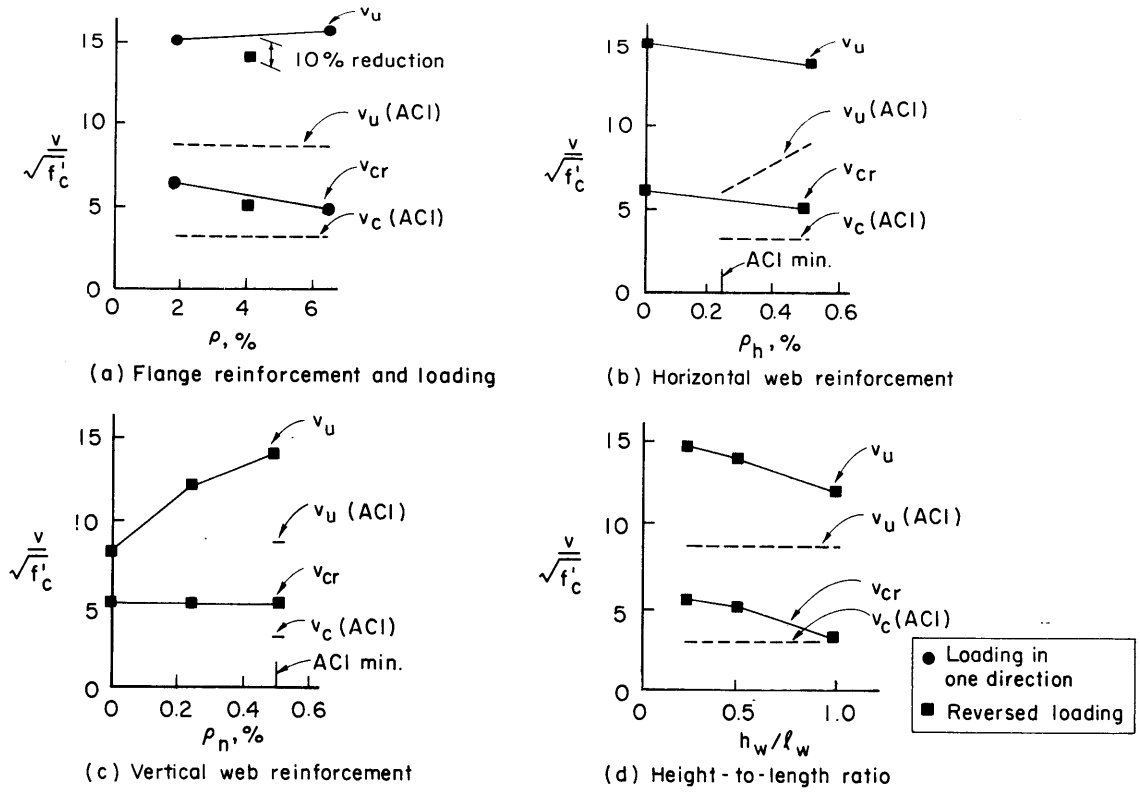

Fig. 5--Effect of principal variables

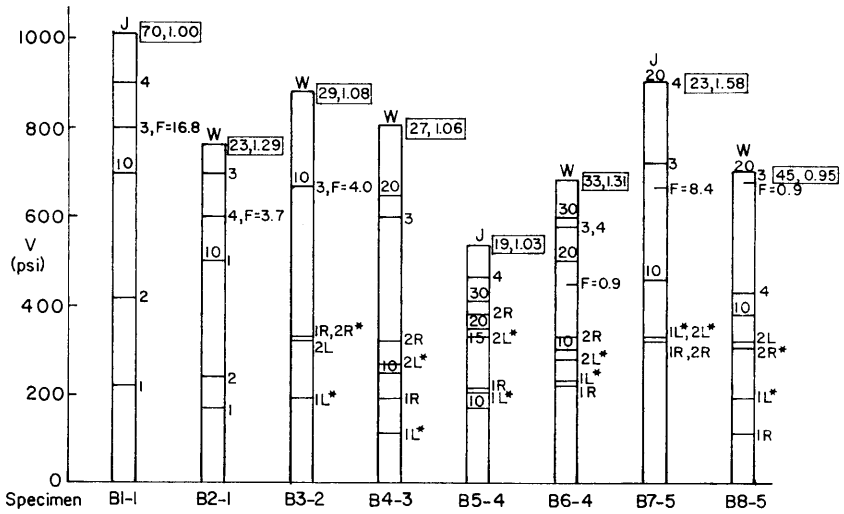

1"= 25.4 mm

1000psi = 70.3 kg/sq. cm

Details of specimens are given in Table 1.

1 = First Observed Crack
2 = First Shear Crack
3 = Yield of Vertical Wall Bars
4 = Yield of Horizontal Wall Bars

L = Loading from left
R = Loading from right

*Observed before cracking in other direction

10, 20, 30 = Nominal shear stress at cracks, widths of 0.01, 0.02, and 0.03 in.

F = Ratio of strain in vertical wall reinforcement to strain in horizontal wall reinforcement

29, 1.08 = Average stress in flange reinforcement = 29 ksi, Ratio of measured to stress calculated by simple beam theory = 1.08

W = Distress observed in middle 1/3 of height of the wall

J = Distress observed at top construction joint

Fig. 6--Summary of test results

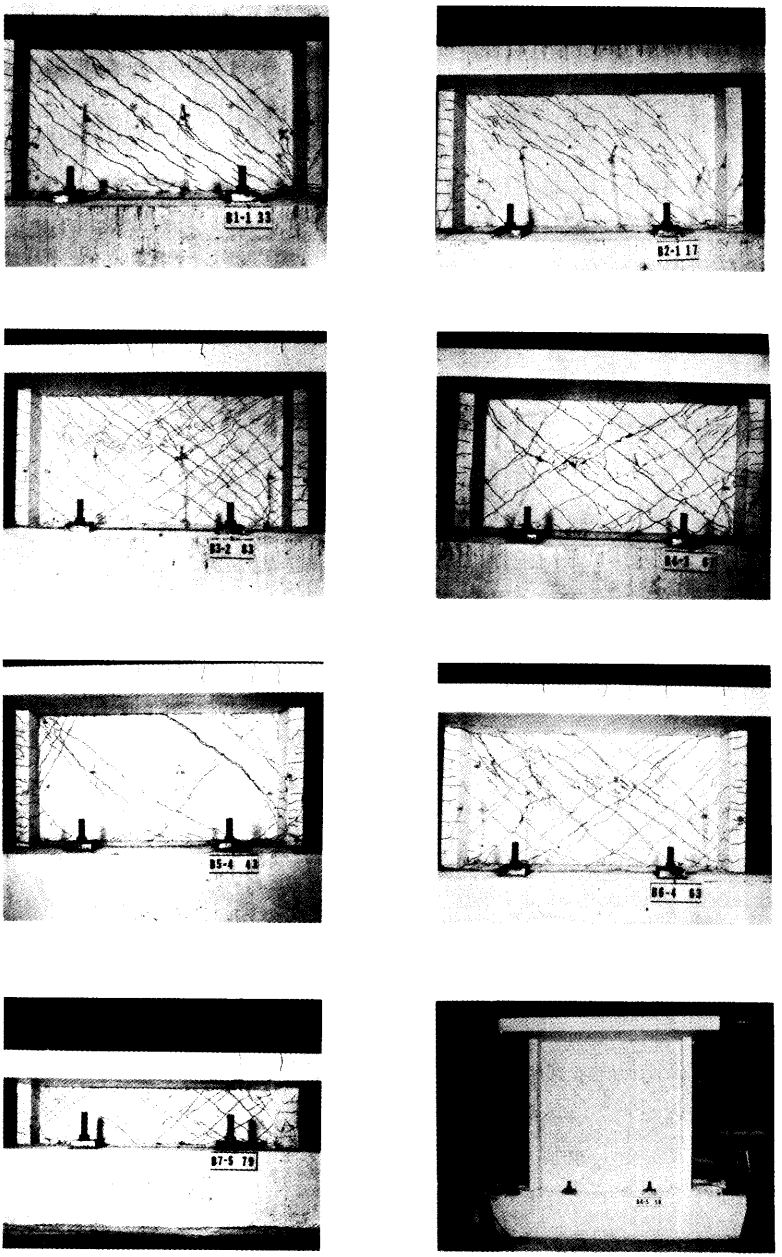

Fig. 7--Photographs of all test specimens at ultimate load

B1-1

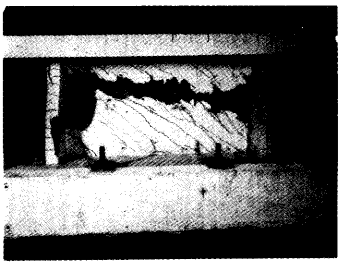

B2-1

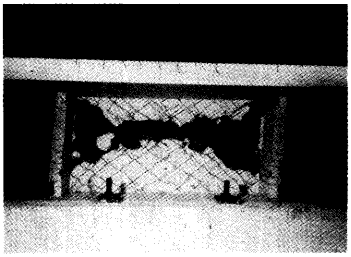

B3-2

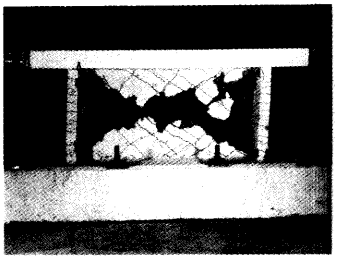

B4-3

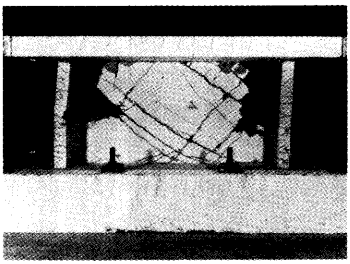

B5-4

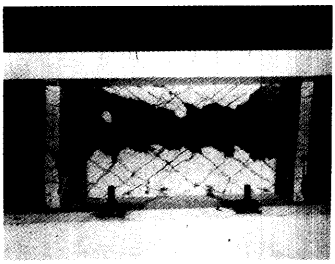

B6-4

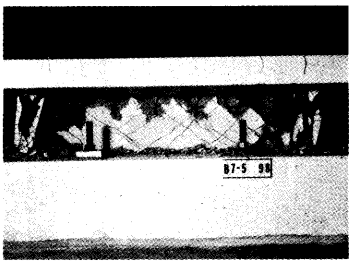

B7-5

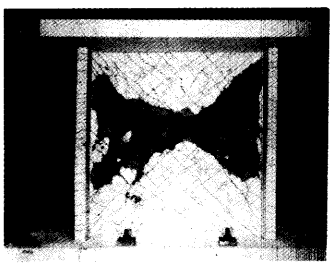

B8-5

Fig. 8--Test specimens at conclusion of loading

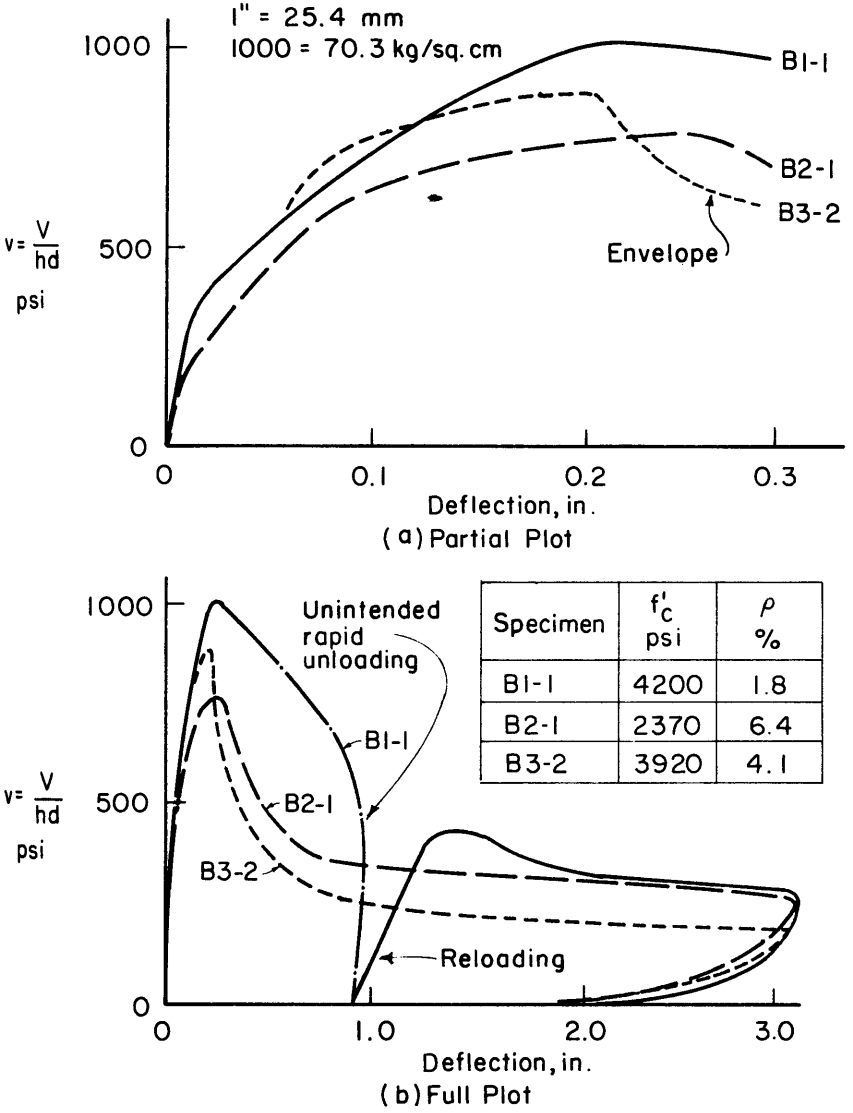

Specimen	f'_c psi	ρ %
B1-1	4200	1.8
B2-1	2370	6.4
B3-2	3920	4.1

Fig. 9--Deflection of B1-1, B2-1, and B3-2

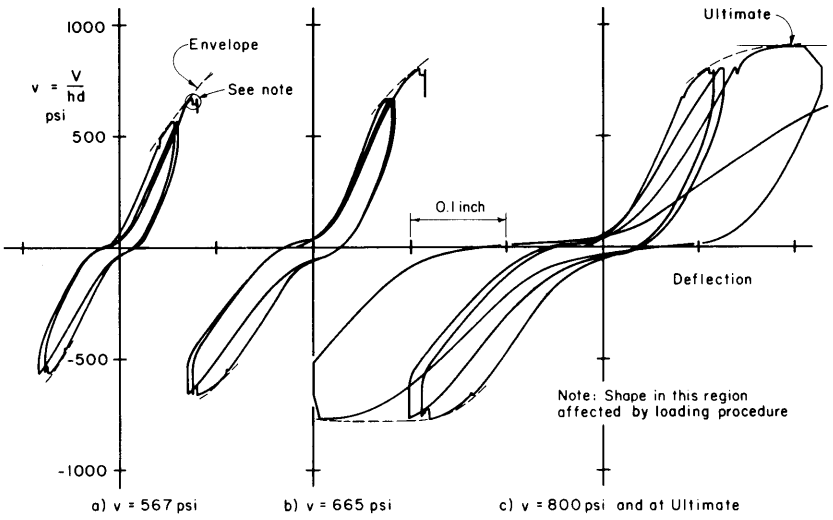

(a) Prior to Ultimate Load

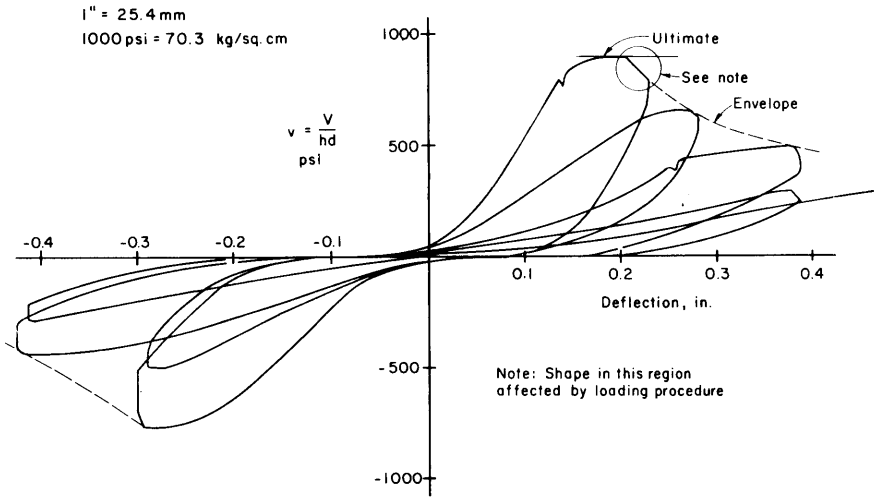

(b) Beyond Ultimate Load

Fig. 10--Measured load versus deflection relationship of B3-2

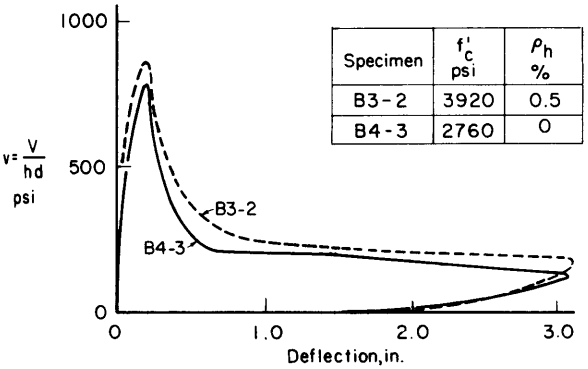

Specimen	f'_c psi	ρ_h %
B3-2	3920	0.5
B4-3	2760	0

1" = 25.4 mm
1000 psi = 70.3 kg/sq. cm

Fig. 11--Deflection envelopes of B3-2 and B4-3

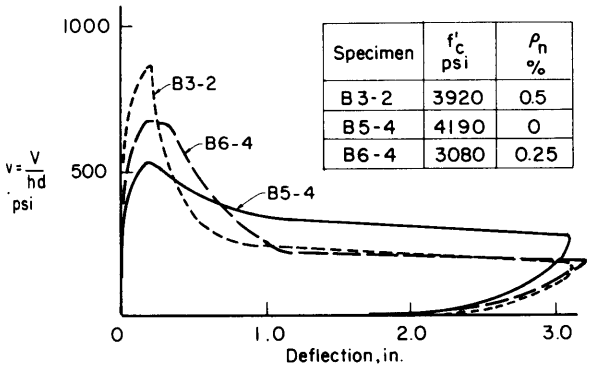

Specimen	f'_c psi	ρ_n %
B3-2	3920	0.5
B5-4	4190	0
B6-4	3080	0.25

1" = 25.4 mm
1000 psi = 70.3 kg/sq. cm

Fig. 12--Deflection envelopes for B3-2, B5-4, and B6-4

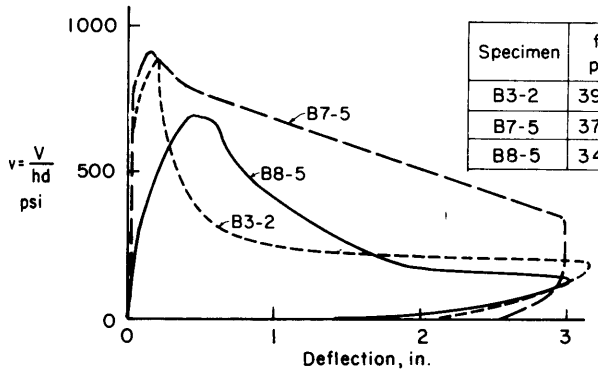

Specimen	f'_c psi	h_w/ℓ_w
B3-2	3910	$\frac{1}{2}$
B7-5	3730	$\frac{1}{4}$
B8-5	3400	1

1" = 25.4 mm
1000 psi = 70.3 kg/sq. cm

Fig. 13--Deflection envelopes of B3-2, B7-5, and B8-5

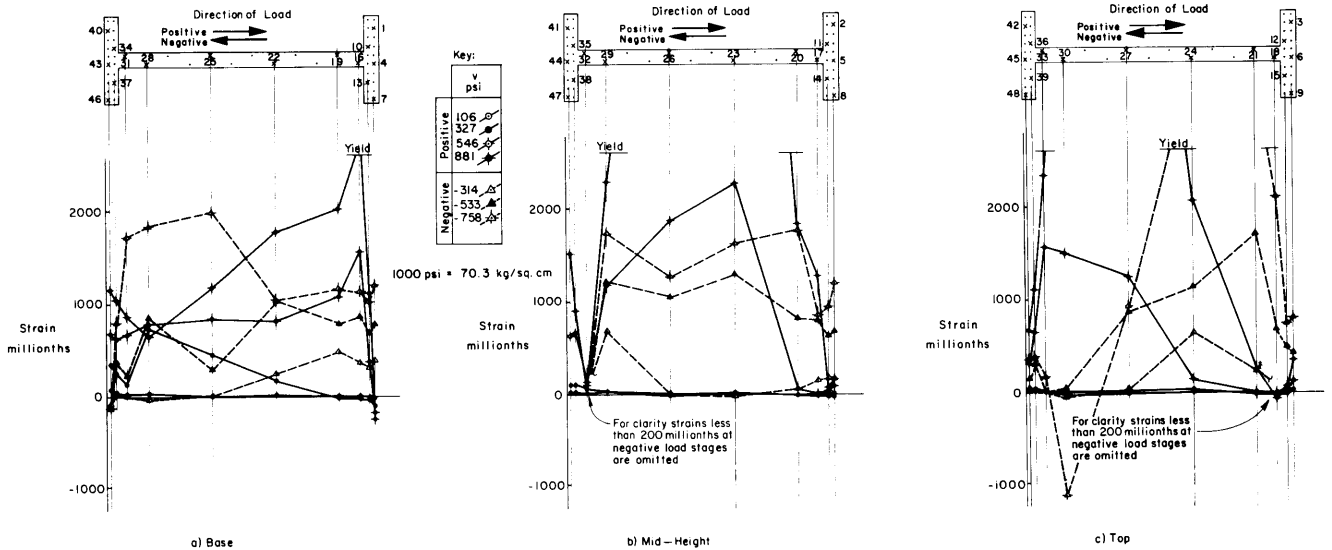

Fig. 14--Vertical strain in B3-2

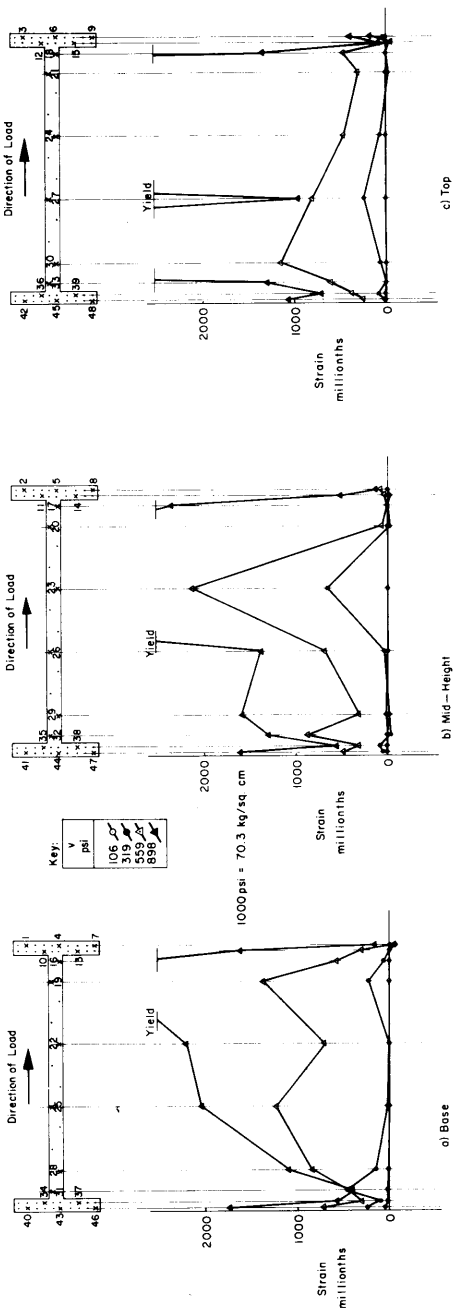

Fig. 15--Vertical strain in B7-5

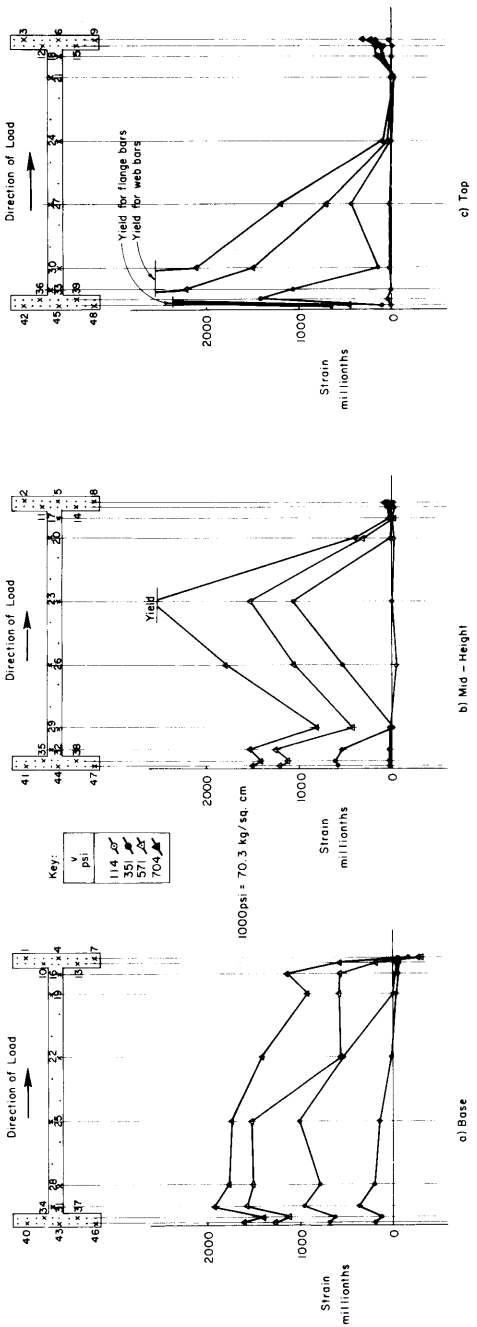

Fig. 16--Vertical strain in B8-5

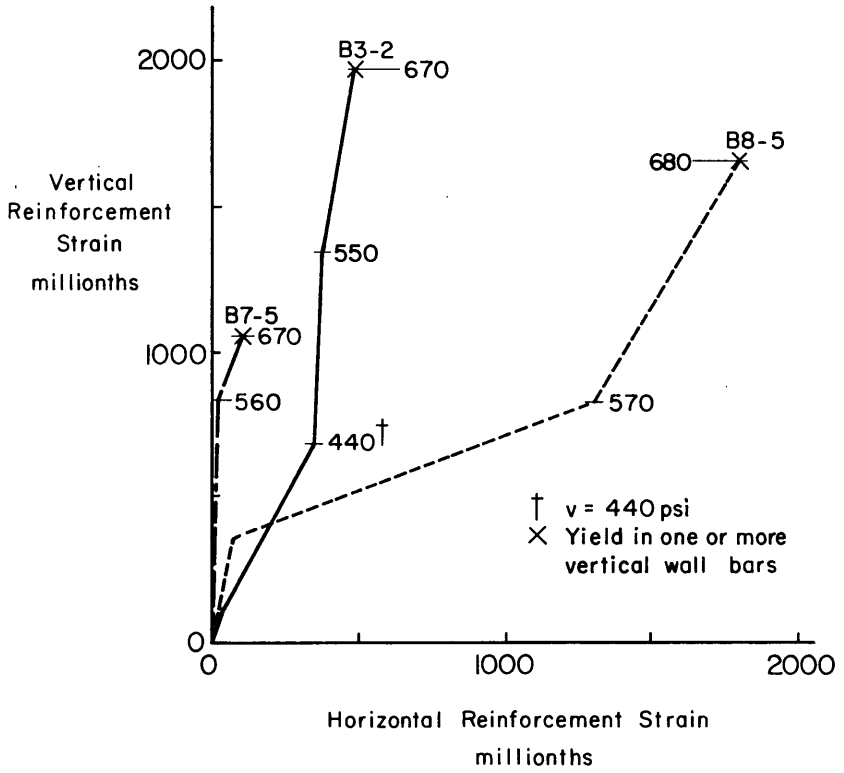

1000 psi = 70.3 kg/sq. cm

Fig. 17--Comparison of wall strains for B3-2, B7-5, and B8-5

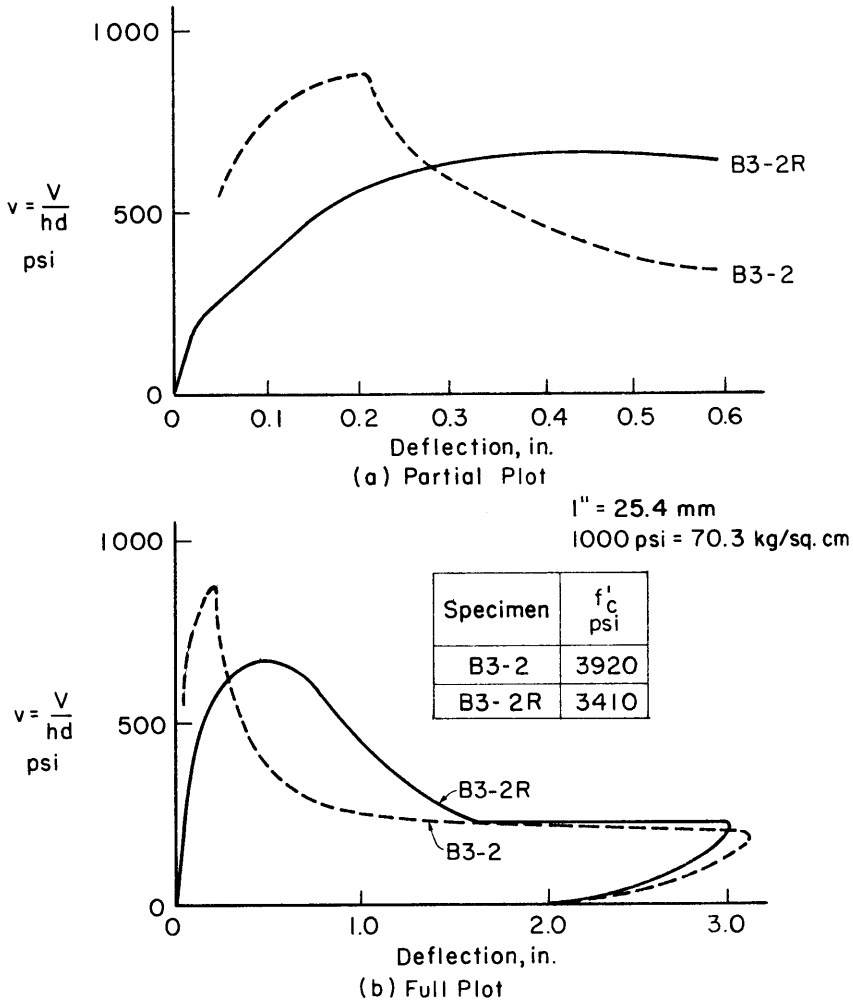

Fig. 18--Deflection envelopes of B3-2 and B3-2R

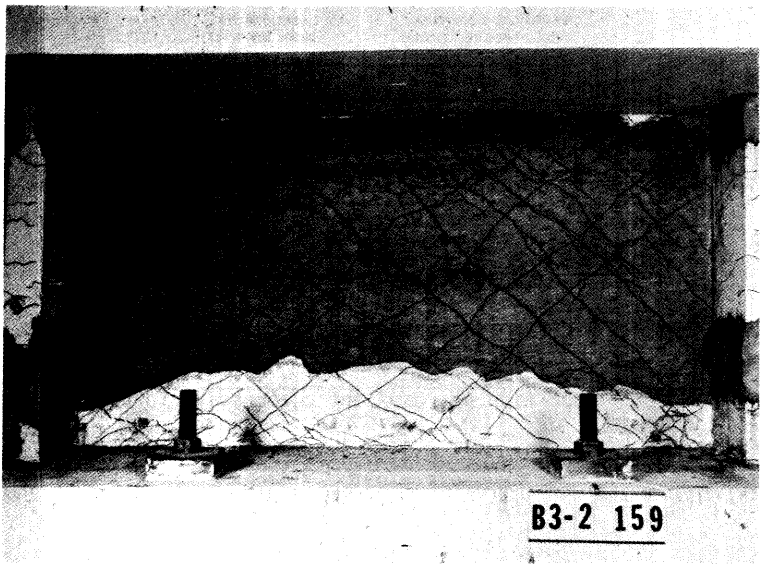

Fig. 19--Specimen B3-2R at ultimate load

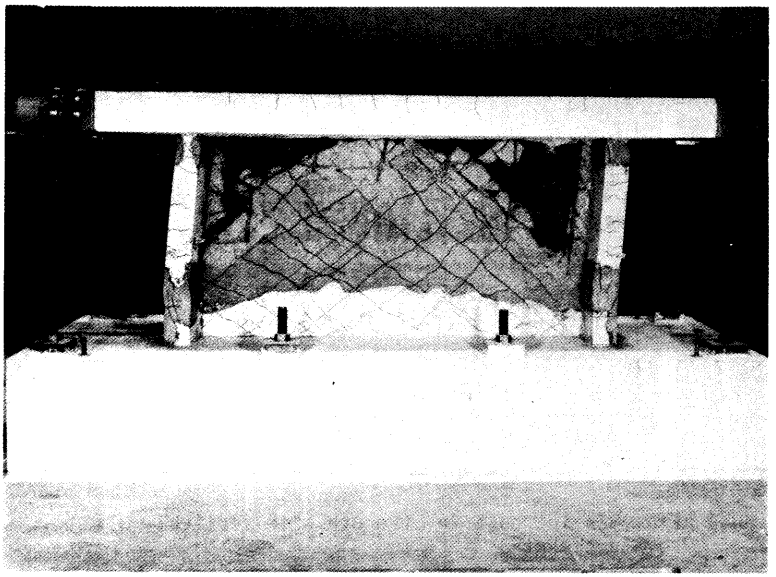

Fig. 20--Specimen B3-2R at end of test

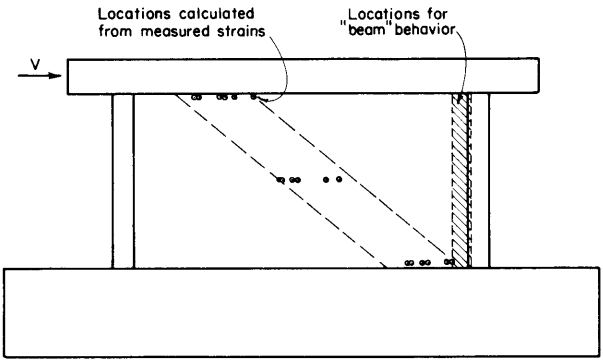

Fig. 21--Location of resultant compressive force in concrete

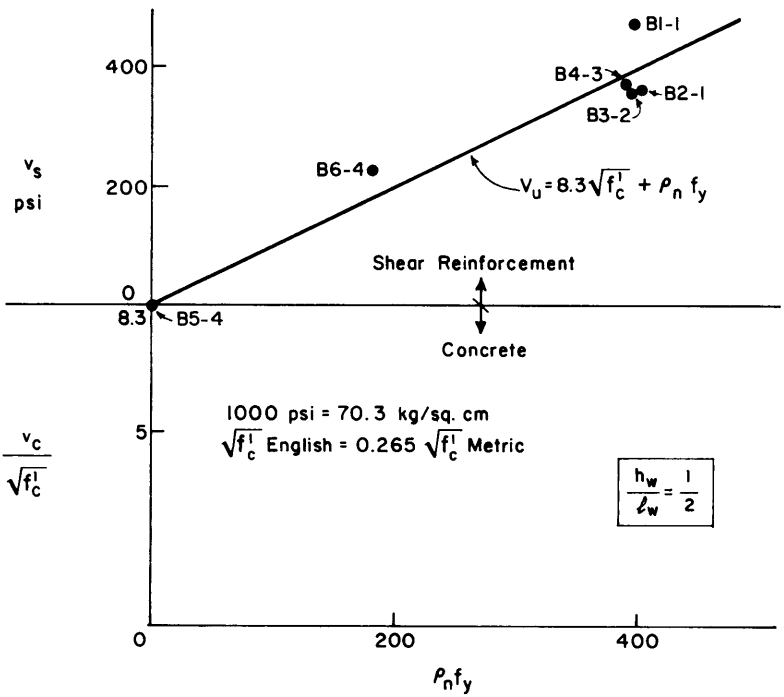

Fig. 22--Increase in strength with vertical wall reinforcement

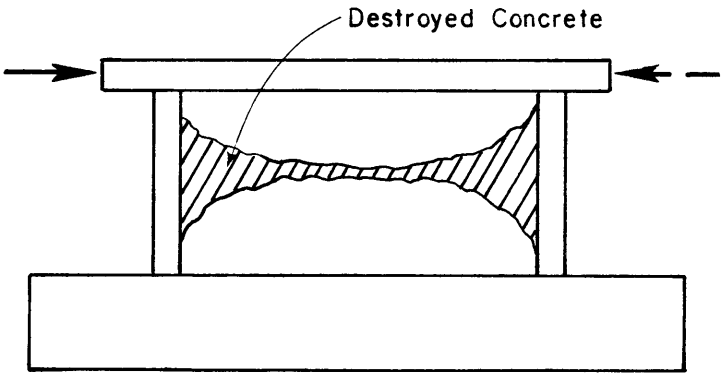

(a) Specimen at End of Test

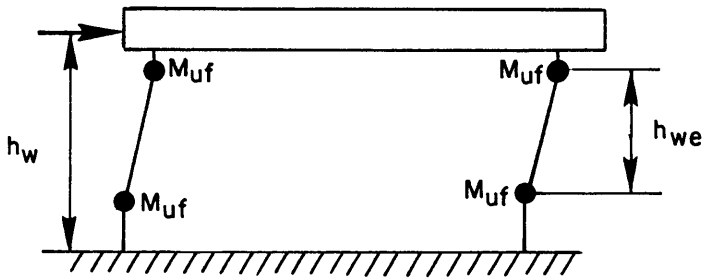

(b) Idealized Frame Action

Fig. 23--Frame action beyond ultimate

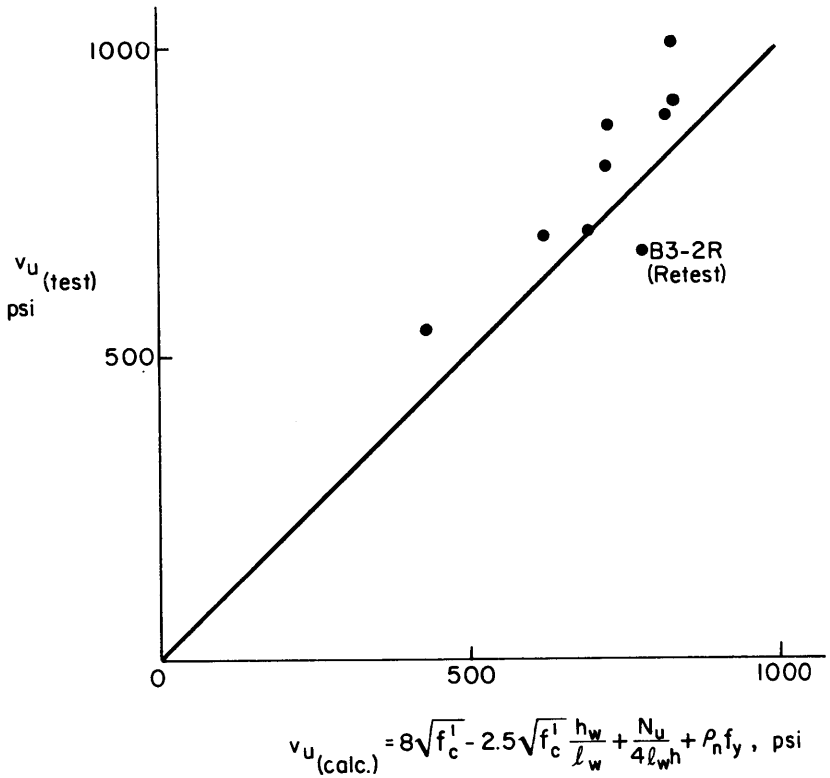

Fig. 24--Tests calculated versus shear stress